LM-07K001b
March 19, 2007

Tandem Filer Development for Thermophotovoltaic Energy Conversion from January 2003 to February 2006

PM Fourspring

Tandem Filter Development for Thermophotovoltaic Energy Conversion from January 2003 to February 2006

P. M. Fourspring
Advanced Concepts – Energy Conversion Technology
Advance Reactors Program
KAPL, Inc., a Lockheed Martin Company

Report Number: ARP-AC-1326-E2

October 2006

This Page Intentionally Blank

ACKNOWLEDGEMENTS

The initiatives and progress described in this report augmented an ongoing and highly successful development program for thermophotovoltaic spectral control. Many individuals contributed to these initiatives and the progress, and specific, individual contributions to this development program are named or referenced in the report.

Several individuals made significant, general contributions to various aspects of the program and as such are not named or referenced. Dave DePoy contributed valuable knowledge about all aspects of the development program including lessons from the past development efforts. Lee Danielson worked with me through the difficult and tedious assessment of the FT-IR spectrometer, and Lee along with Josef Parrington worked with me over a long stretch of every other Friday mornings to assess the dispersive spectrometer. Todd Lavery completed over 2500 spectral reflectance or transmittance measurements of material samples and tandem filters and had to endure numerous procedural changes for these measurements. Finally, John Azarkevich made numerous miscellaneous contributions and completed the vacuum oven baking of the material samples and tandem filters for the time-at-temperature testing.

This Page Intentionally Blank

TABLE OF CONTENTS

INTRODUCTION

The intent of this report is to summarize the tandem filter development for spectral control of thermophotovoltaic energy conversion from January 2003 to the termination of the program in February 2006 and to closeout tandem filter development in order to capture the knowledge gained from the development effort.

Over the last three years, the goals of the tandem filter development have been the following:

- Study the limits of the design of the interference optical coatings component of a tandem filter in order to develop higher performance designs,
- Enhance the fabrication process of the optical interference coatings to increase the fidelity with the intended design and allow more complex, higher performing designs,
- Support TPV module testing by providing tandem filters and assembly assistance,
- Identify and develop materials for optical interference coatings that are stable at higher temperatures than current materials,
- Improve the understanding of the directional and spectral reflectance and transmittance characterization of the completed tandem filters to insure the veracity of the characterization data and to provide useful feedback to the tandem filter development process.

This development effort has been a collaboration between KAPL and its contracted development partner, Rugate Technologies Inc.

CONCLUSIONS

In the near term, additional improvement in tandem filter performance is possible. Significant improvement in the Sb_2Se_3 based tandem filters will only occur with the identification of new design spaces that yield a significantly improved design that can be fabricated. Otherwise, the fidelity of the fabrication process to the design is within a few percent overall, and hence no significant improvement is possible with the current designs. On the other hand, the GaTe based tandem filters have not yet achieved the same level of fabrication fidelity with the difference between the design and the fabricated tandem filter on the order of 20%. The expectation is that further fabrication development will close this gap and the GaTe based tandem filters will then also be limited by the current designs.

No additional performance improvement is expected for the plasma filter component of the tandem filters.

RECOMMENDATIONS

Continued development of thermophotovoltaic spectral control should focus on the optical interference coatings used for the tandem filters in the near term. First, continue fabrication development of the GaTe based tandem filters to improve fabrication fidelity. Second, to determine if additional design space for tandem filters exist, continue development of fundamental design understanding of optical interference coatings. Third, continue development of alternative materials for use in the optical interference coatings.

PROGRAM ACHIEVEMENTS

The primary achievements of the tandem filter development program were as follows:

- **Increased Performance of Tandem Filters**

  A 0.60 eV (nominal) tandem filter was used to achieve a new world record of 22.1% at reference conditions for TPV efficiency (Reference (1)). Moreover, the tandem filters alone yielded the 10% increase in efficiency over the previous world record of 20% since the measured performance of the TPV cell used was slightly lower than the TPV cell used for the 20% efficiency measurement (Reference (2)). Furthermore, comparing best-to-best, the spectral efficiency of fabricated tandem filters advanced 6% (78.9% to 83.7%) for the 0.52 eV filters and 7% (72.7% to 77.9%) for the 0.60eV (nominal) filters from the values reported prior to January 2003.

- **Identified and Developed an Alternative, High Index Material for Greater Temperature Stability of Tandem Filters**

  The identification and development of an alternative, high index material that is stable at higher temperatures than Sb_2Se_3 (the current, high index material) was achieved. GaTe was identified as a potentially applicable material that is stable at higher temperatures and was developed to achieve a viable tandem filter that has been fabricated successfully numerous times. The temperature stability of the GaTe based tandem filters have been demonstrated to 302F (150C) for over 1000 hours as compared to the Sb_2Se_3 based tandem filters that are only stable at 176F (80C) or less for over 1000 hours. Although the index of refraction is slightly lower for the GaTe material, the design performance of the GaTe based tandem filters is within 5% of the Sb_2Se_3 based tandem filter.

- **Developed an Alternative Design Configuration for Tandem Filters**

  A new tandem filter design configuration (cell defined edge) was developed, tested, and selected to maintain the spectral performance while enhancing the above band gap transmission performance and hence the power density performance of a TPV module.

- **Reduced Fabrication Variability of Tandem Filters**

  The standard deviation of the filter edge location, spectral efficiency, and above band gap transmission was reduced 50% from the previous class of tandem filters. Although no studies have conclusively determined how each modification contributed to the decrease in fabrication variation, the expectation is that all modifications contributed.

  In addition, the standard deviation of the filter edge location across a fabricated tandem filter was reduced from 8-10% to less than 1.5% for 3 inch diameter wafers and reduced from 2-3% to less than 1.0% for 2 inch diameter wafers. This reduction in variation across a filter was a direct result of an addition of a mask to the physical vapor deposition chamber. As a result, the standard deviations of the filter edge location, TPV efficiency, and TPV power density are insignificant assuming a perfectly uniform TPV cell.

- **Completed a Set of Sustained Fabrication Runs of Tandem Filters**

  A sustained production of tandem filters was achieved for the first time to support the fabrication of a 50 W small array test. The sustained production included the successful completion of 11 fabrication runs of 4 tandem filters each for a total of 44 filters. The importance of this demonstration was twofold. First, the sustained production showed that the fabrication process could reliably operate over an approximate six week time period with back-to-back runs. Second, sustained production provided an indication of fabrication process variation both within and between runs.

Some 125 tandem filters were fabricated and characterized along the way in reaching these achievements. The following sections provide details of these achievements and the initiatives that led to the achievements.

PROGRAM INITIATIVES

Numerous development initiatives were formulated and implemented to achieve the development program goals listed previously. Specifically, these initiatives include the following:

- Design of Optical Interference Coatings
    - Development of the cell defined edge configuration,
    - Development of a specialized optical interference coatings optimization code,
    - Development of an approach and techniques to understand and explore the design space for optical interference coatings
- Fabrication of Optical Interference Coatings
    - Fabrication of tandem filter that enabled a new TPV efficiency record,
    - Fabrication of a tandem filter set to support first small array test,
    - Fabrication of higher performing tandem filters,
    - Fabrication of three classes of tandem filters,
    - Development of an approach to increase fabrication fidelity,
    - Implementation of sustained fabrication of tandem filters,
    - Modification of fabrication system to improve deposition uniformity,
    - Modification of fabrication system cooling,
    - Implementation of source conditioning procedures,
    - Implementation of an alternative technique for evaporation of source materials,
    - Optimization of substrate temperature and deposition rate,
    - Enhancement of fabrication operating procedures
- Material Development for Optical Interference Coatings
    - Identification of an alternate, high index material for the optical interference coatings,
    - Characterization of the instantaneous transformation temperature of all the materials used in the optical interference coatings,
    - Characterization of the time-at-temperature capability of the Sb_2Se_3 and GaTe based tandem filters,
    - Fabrication trial of co-deposition of Sb_2Se_3 and Sb_2S_3
- Fabrication of Plasma Filters
    - Fabrication of multiple, three inch diameter plasma filters,
    - Fabrication of plasma filters with lower doping levels
- Optical Characterization of Tandem Filters
    - Implementation of periodic evaluations of the Au working standard for reflectance measurements using the FT-IR spectrophotometer,
    - Assessing the spectral and directional reflectance of the Au standard,
    - Assessing the limitations of optical characterization with random polarization,

  - Assessing the limitations of the fourier transform infrared (FT-IR) spectrometer,
  - Assessing the limitations of the dispersive spectrometer

- TPV Module Fabrication Using Tandem Filters

  - Development of trimming techniques and an adhesive application system for the fabrication of TPV modules using tandem filters,
  - Identification of the potential cause of TPV module failures at the TPV cell / tandem filter interface

- Outreach for Optical Interference Coatings Knowledge

These initiatives are described in the following sections. Many of these initiatives supported or directly yielded the program achievements listed previously. Other program initiatives were incomplete at the time of the program termination; and instead of describing the results, a status of these initiatives is provided.

Design of the Optical Interference Coatings

The design of optical interference coatings establishes, in general, the limiting performance of the fabricated, optical interference coatings. Therefore, the performance of optical interference coatings is limited first by the performance of the design of the coatings and second by the fidelity of the fabrication process in creating the design. The intent of the initiatives discussed in this subsection was to increase the performance of the designs in order to increase the performance of the fabricated optical interference coatings. A later subsection will discuss the initiatives to improve the fidelity of the fabrication of the optical interference coatings.

<u>Development of a Specialized Optical Interference Coatings Optimization Code</u>

Rugate Technologies, Inc. developed a tandem filter design code referred to as ‘Dispersion’ that optimizes the design of the optical interference coatings component of tandem filters for both spectral efficiency and above band gap transmission performance criteria. The commercial design codes for optical interference coatings typically optimized based on a desired shape of the spectral and directional reflectance and transmittance. (Note, both are necessary to specify in order to include the effect of the absorption in the materials used to create the optical interference coatings.) The intent of this development was to achieve higher tandem filter performance by directly optimizing the optical interference coatings on the spectral control figures of merit rather than indirectly optimizing the coatings on the desired shape of the spectral and directional reflectance and transmittance.

Using Dispersion together with variations of the basic design architecture, Rugate Technologies, Inc. achieved higher performing optical interference coatings as shown in Table 1.

Table 1 Comparison of Optical Interference Design Performance*

		Current	Previous	Δ* (%)
0.52 eV	$\eta_{spectral}$ (%)	84.1	79.3	6.1
	$T_{>Eg}$ (%)	81.1	78.4	3.4
	No. Layers	69	52	
	ID	767	52 Layer	
0.60 eV (nominal)	$\eta_{spectral}$ (%))	78.6	74.8	5.1
	$T_{>Eg}$ (%)	80.1	82.8	(3.3)
	No. Layers	69	58	
	ID	767	58 Layer	

* The performance values are for radiating surface temperature of 1750°F with a blackbody emissivity and no water absorption in the incident layer of YF_3 (see text for a description).

Before continuing with the discussion about the development of the design code, a brief digression to explain the design performance values presented in Table 1 is appropriate. In general, the performance values shown for each design represent the highest achievable performance for the design. The material properties used to predict the performance of a design are measured properties from samples of each material deposited with the same fabrication process used to create the tandem filters. However, the material properties can vary due to both known and unknown causes, and the variations usually degrade performance. For example, Figure 1 shows the impact of water absorption in the exterior layer of YF_3 on the spectral reflectance and the performance of a tandem filter design. This absorption does not occur to the same extent for every tandem filter. The spectral reflectance and performance of a comparable, fabricated tandem filter are also shown in Figure 1. The spectral reflectance of the fabricated filter falls between the reflectance of the filter design with and without water absorption. The water absorption can degrade the performance of the tandem filter design by 6-7%. This example is extreme; other material property variations would not necessarily yield such a large degradation. So, rather than trying to anticipate variations in the material properties (like water absorption), the performance values shown for a given design represent the highest achievable performance for the design.

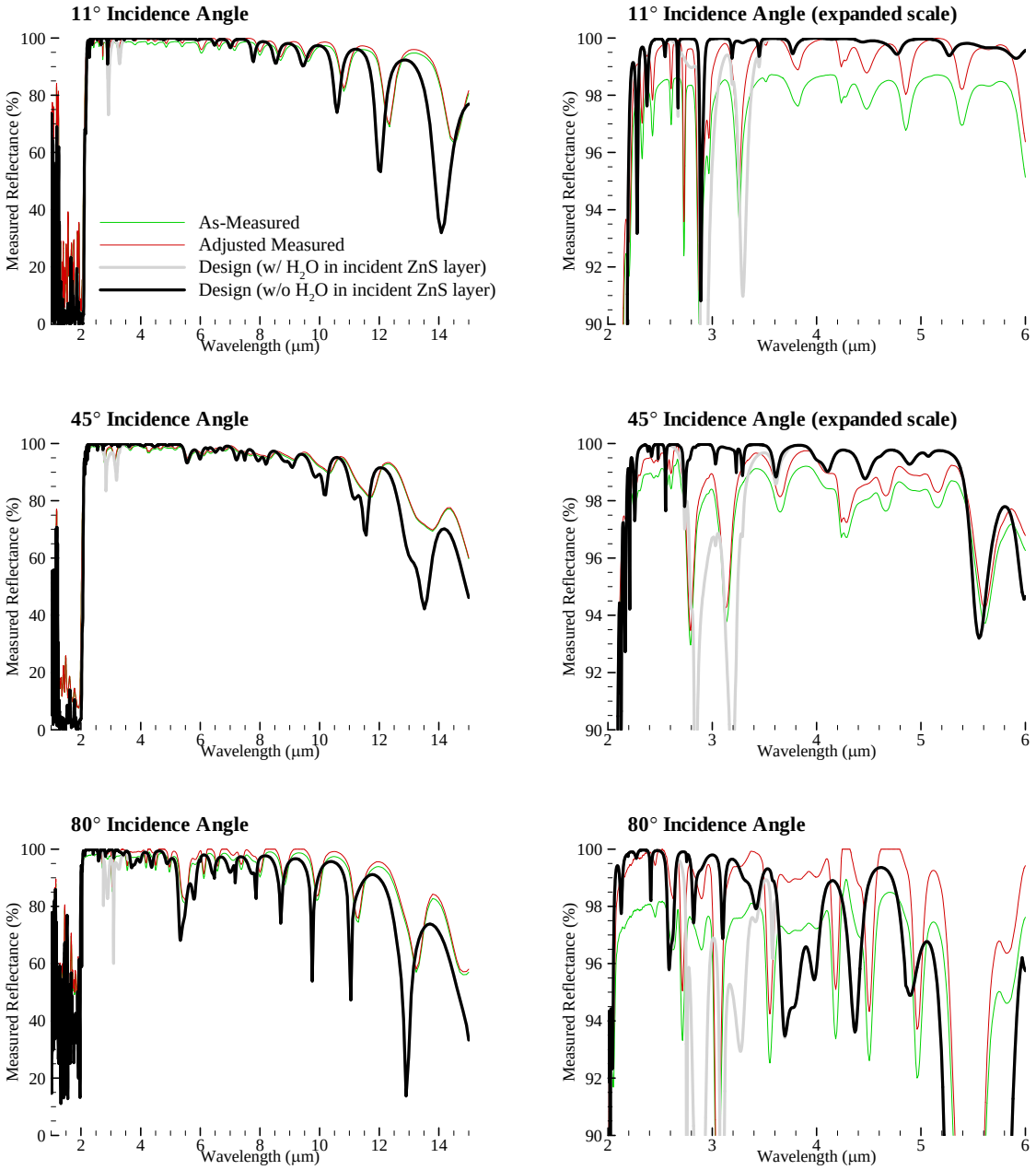

	Fabricated*		Design	
	adjusted	as-measured	w/o H_2O*	w/ H_2O
$\eta_{spectral}$ (%)	77.9	75.7	78.6	73.5
$T_{>Eg}$ (%)	72.6	72.9	80.1	79.5
Edge (μm)	2.01	2.01	2.07	2.07
ID	KX12		767	

* Adjusted Value / As-Measured represent two values of the performance for spectral efficiency and above band gap transmission due to the uncertainty associated with the optical characterization as discussed later in this report.

Figure 1: Comparison of the Spectral Reflectance of a Tandem Filter Design and a Fabricated Tandem Filter Using the Design

No studies to conclusively determine what portion of the higher performance can be attributed to the design code vice the changes in the basic architecture have been completed. Moreover, a few comparisons of the optimization by Dispersion to the optimization by a commercial code both beginning with the same initial design showed that the commercial code could achieve similar results as Dispersion. For example, Table 2 shows a comparison of the optimization results for a key design, referred to as the 767 design, proposed by Rugate Technologies, Inc. for a 0.60eV (nominal) band gap filter and 1750F radiating surface.

Table 2: Design Code Comparison for Optimization of Optical Interference Coatings*

Case (0.60eV (nominal)	$\eta_{spectral}$	$T_{>Eg}$	Number of Layers	Edge (μm)	Thinnest Layers (μm)
767 Initial Design	70.2	75.3	69	2.08	0.500
Dispersion (via refinement) (Rugate Technologies Inc.)	73.8	79.7	69	2.07	0.0382
Optilayer (via refinement) (Commercial Code)	73.1	80.7	69	2.08	0.0871
Δ Codes (%)	(0.95%)	+1.3%	—	—	—

* The spectral efficiency values are lower than fabricated values reported in the previous table. The values shown in this table assumed water absorption in the exterior layer of the optical interference coatings as discussed in the text.

As shown in this table, Dispersion increased the performance of the initial design through refinement. The initial design was not developed using computer optimization but rather represents an architecture based on design knowledge. Refinement, in general, refers to the use of optimization algorithms for optical interference coatings that change the thicknesses of the layers to increase performance based on a given criteria. With both optimization codes shown in Table 2, the structure (arrangement) of the layers is maintained, only the thicknesses of the individuals layers changed.

The spectral efficiency increased 5.1% and the above band gap transmission increased 5.8% from the initial design. Similarly, the commercial Optilayer code increased spectral efficiency by 4.1% and above band gap transmission by 7.2% through refinement but using a reflectance and transmittance based criteria rather than the spectral control figures of merit. For the example in Table 2, the Dispersion code optimized the design with a higher spectral efficiency than the design optimized by the Optilayer code, but the Optilayer code created a design with a higher above band gap transmission than the design created by Dispersion. For both codes, the criteria used in the optimization could be adjusted to emphasize spectral control over above band gap transmission or vice versa. Therefore, both codes can enhance the performance of an initial design through refinement and are complementary.

In the end, Dispersion was successful as it was used to optimize the 767 tandem filter class and the subsequent G class tandem filter. Furthermore, only Dispersion could be adapted to optimize the cell defined edge configuration as described in the next section. Therefore, Dispersion, Optilayer, and perhaps other design codes should be used together to achieve the highest performing optical interference coatings for tandem filters.

Finally, the relatively high performance of the initial design prior to refinement shown in Table 2 suggests the importance of the basic architecture of the design. The design architecture captures the knowledge obtained over the several years of development of the tandem filter for TPV spectral control. To be sure, both design codes improved the initial design and are invaluable tools in the design process. However, the design codes typically have little success in dramatically improving a low performing, initial design. Therefore, knowledge of optical interference coatings is critical to the design process as will be described next.

Development of the Cell Defined Edge Configuration

The cell defined edge configuration alters the design space for the optical interference coatings on the incident surface of the tandem filters. This configuration shifts the edge between the low reflection and the high reflection of the optical interference coatings to a longer wavelength. Instead of attempting to reflect all the below band gap photons with the tandem filter, the cell defined edge configuration allows some of the below band gap photons to pass into the cell. The TPV cell then sorts the below and above band gap photons and reflects the below band gap photons with the back surface reflector.

In contrast, with traditional tandem filter configurations, the tandem filter defines the edge between the low reflection and the high reflection and thus the edge between above band gap (convertible) and below band gap (nonconvertible) photons to minimize the transmittance of below band gap photons to the TPV cell. As a result, above band gap photons can be inadvertently reflected since the band gap of a TPV cell varies with temperature and cell to cell.

A key design requirement for the optical interference coatings with the tandem filter defined edge is the sharpness and location of the edge between the low reflectance and the high reflectance regions. With the cell defined edge configuration, the importance of the sharpness and the location of this edge may be reduced, altering the design space for the optical interference coatings. Both of these changes may ease the design of the optical interference coatings. As a result the designs of the optical interference filters can focus on further improving the pass band (low reflection region) to increase power density and to a lesser extent further improving the magnitude of the reflection in the rejection band (high reflection region) to increase the efficiency.

The optimal location of the tandem filter edge has been evaluated since the beginning of front surface, spectral control development. This consideration continued in 2003 with Paul F. Baldasaro asking if the performance of the back surface reflector could be improved further and what is the optimum position of the tandem filter edge relative to the reflectance contribution by the back surface reflector. The modeling and experimental testing culminated in 2005 with the decision to change to a cell defined edge configuration. Modeling and experimental verification of the advantage of the cell defined edge configuration has been completed. Key to the change to the cell defined edge configuration was the development of a coupled model of the tandem filter and the TPV cell by David M. DePoy that allowed the assessment of the configuration. All tandem filters fabricated since September 2005 have been designs with the cell defined edge configuration.

Using this coupled model, the design space for the cell defined edge configuration for 0.6 eV (nominal) TPV cells is show in Figure 2. Using idealized values of spectral reflectance and transmittance for incident angles of a tandem filter, the design space was mapped by systematically varying the location and slope of the tandem filter edge (the transition from low reflectance to high reflectance).

As expected, the maximum predicted efficiency occurs at approximately 2.08µm with a sharp transition to high reflectance (see A=2.08 and B=2.09 in Figure 2). The 2.08µm wavelength is approximately the edge of the TPV cell band gap. At this wavelength, the tandem filter is providing the majority if not all of the reflectance of below band gap photons as compared to the reflection of below band gap photons by the back surface reflector. As suggested in Figure 2, optimum design would seem to have an edge between above band gap (convertible) and below band gap (nonconvertible) photons of 2.09-2.10µm (see A=2.08 and B=2.09-2.11 in Figure 2).

To determine the intersection of the design space for efficiency and for power density, Rugate Technology, Inc. ported the coupled model of the tandem filter and the TPV cell into their tandem filter design code (described further in the next section). The design of the optical interference coatings for the tandem filter was then optimized for the cell defined edge configuration and the results are shown in Table 3.

Predicted TPV Efficiency

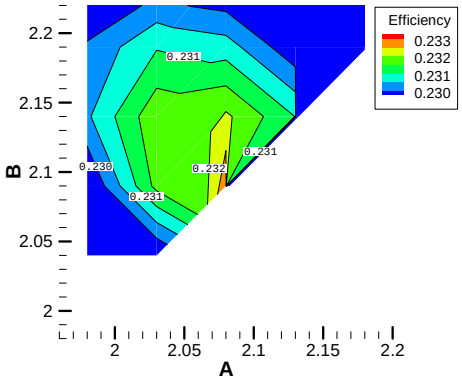

Predicted TPV Power Denisty

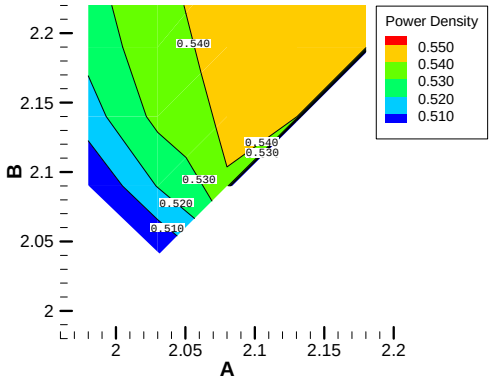

Tabulated Results

A	B	Efficiency	Power Density	Edge
1.98	2.04	0.2268441	0.4775	2.01
1.98	2.09	0.2294503	0.4998	2.035
1.98	2.14	0.2304168	0.5155	2.06
1.98	2.19	0.2300852	0.5232	2.085
1.98	2.30	0.2278844	0.5311	2.14
2.03	2.04	0.2294589	0.4989	2.035
2.03	2.09	0.2316526	0.5205	2.06
2.03	2.14	0.2318727	0.5328	2.085
2.03	2.19	0.2309576	0.5369	2.11
2.03	2.30	0.2281016	0.5403	2.165
2.08	2.09	**0.2329184**	0.5386	2.085
2.08	2.14	0.2320976	0.5437	2.11
2.08	2.19	0.2307465	0.5443	2.1349
2.08	2.25	0.2289983	0.5445	2.165
2.08	2.30	0.2274999	0.5446	2.19
2.13	2.09	0	0	0
2.13	2.14	0.2309901	0.5445	2.135
2.13	2.19	0.2296041	0.5447	2.16
2.13	2.25	0.2278488	0.5448	2.19
2.13	2.30	0.2263504	0.5448	2.215
2.18	2.09	0	0	0
2.18	2.14	0	0	0
2.18	2.19	0.2284291	0.5447	2.185
2.18	2.25	0.2266735	0.5448	2.215
2.18	2.30	0.2251851	0.5448	2.24

Assessment Description

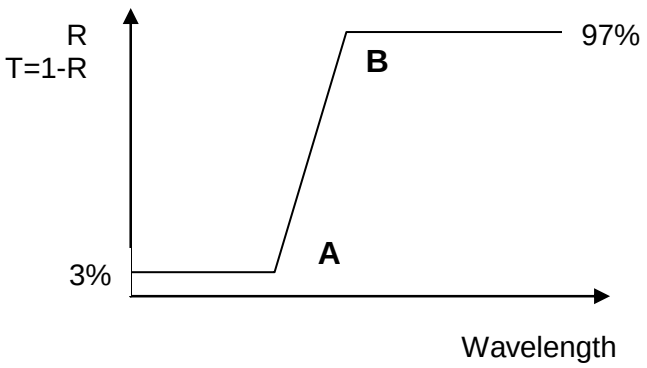

For the reflectance and transmittance shown, the wavelength values of ‘A’ and ‘B’ were methodically varied to map the design space associated with the location and slope of the tandem filter edge. The edge refers to the transition from low reflectance to high reflectance.

Edge = (A+B)/2

Figure 2: Design Space, Cell Defined Edge Assuming HEM9a Performance

Table 3: Performance of the Optical Interference Coatings Designs for the Cell Defined Edge Configuration

Name	η (%)	PD (W/cm^2)	Edge (μm)
G (Sb_2Se_3)	22.1	0.458	2.09
G (GaTe)	20.9	0.488	2.14

The design development is incomplete due to the termination of the TPV development program. From Table 3, the predicted efficiency performance of the Sb_2Se_3 based tandem filters is expected to be slightly better than the GaTe based tandem filters. The predicted power densities shown in Table 3 indicate, however, a higher performance for the GaTe based tandem filters than the Sb_2Se_3 based tandem filters. With additional development, the design of the Sb_2Se_3 based tandem filters should improve and exceed the predicted power density of the GaTe based tandem filters.

Development of an Approach and Techniques to Understand and Explore the Design Space for Optical Interference Coatings

The initial design architecture of the optical interference coatings for the tandem filter is key to the performance of the tandem filters, given that the plasma filter component is assumed to be optimized as described later. The architecture refers to the fundamental arrangement of materials and layer thicknesses to achieve prescribed spectral and directional reflectance, transmittance, and absorptance. The performance of this class of filters is provided later.

To achieve a step change in the performance of the tandem filter configuration, however, a new architecture is likely required for the optical interference coatings. An extensive review of applicable arrangements and layer thickness using the current materials yielded the development plan shown on the following page for the optical interference coatings, which has yet to be fully implemented. To digress briefly, optical interference coatings consist of a series of groupings of thin layers. Each group or component provides a function that sum to provide the overall performance of the coatings as described in Figure 3.

Development Plan:
New, Higher Performing Architecture for the Optical Interference Coatings

Design Alternatives (in recommended order to be explored)

1) Three Material Design Architectures (see Reference (3), Table 5-5)

$AR_{incident}$	$Structure_1$	M_{1-2}	$Structure_2$	M_{2-3}	$Structure_3$	…M_{3-j}	$Structure_j$	AR_{exit}
	AxBxA		AxBxA		AxBxA			
	AxBBxA		AxBBxA		AxBBxA			
			AxBBBxA		AxBBBxA			
			AAxBxAA		AAxBxAA			
					AxBBBBxA			
					AAxBBxAA			

2) Four Material Design Architectures (see Reference (3), Table 5-5)

$AR_{incident}$	$Structure_1$	M_{1-2}	$Structure_2$	M_{2-3}	$Structure_3$	…M_{3-j}	$Structure_j$	AR_{exit}
	AxyBxyA		AxyBxyA		AxyBxyA			
	AxyBBxyA		AxyBBxyA		AxyBBxyA			
			AxyBBBxyA		AxyBBBxyA			
			AAxyBxyAA		AAxyBxyAA			
					AxyBBBBxyA			
					AAxyBBxyAA			

3) Alternative Longer Wavelength, Rejection Band Extensions

- Lower doped InPAs layers (plasma layer)
- Al_2O_3 Substrates instead of InPAs layer

Design Objectives

- Minimize YF3 use to decrease longer wavelength absorption,
- Maximize average index to increase incident angle stability,
- Maximize index contrast to maximize rejection band,

Design Approaches for All Architectures

- Optimization
  - Optimize entire design simultaneously
  - Fix stacks and optimize ARs and match layers only
  - Optimize each stack individually, fix stacks, optimize ARs and match layers only, refine composite design
  - Others …
- Optimization Methods
  - Figure of Merit:: TPV efficiency and power density
    - Steepest descent method
  - Figure of Merit:: Target/Shape based (square of the sum of the differences)
    - Hyper Newton method
    - Modified damped least squares (Modified DLS)
    - Newton method
    - Sequential QP method

Design Constraints

The designs shall constrain physical layers thickness to greater than 100Å or greater than 1000Å (evaluate performance of both) and limit the number of layers to 100. The plasma layer shall be modeled as 1µm thick.

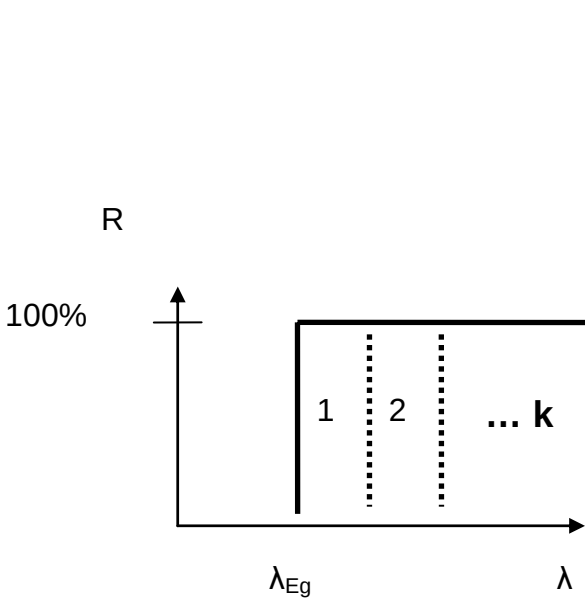

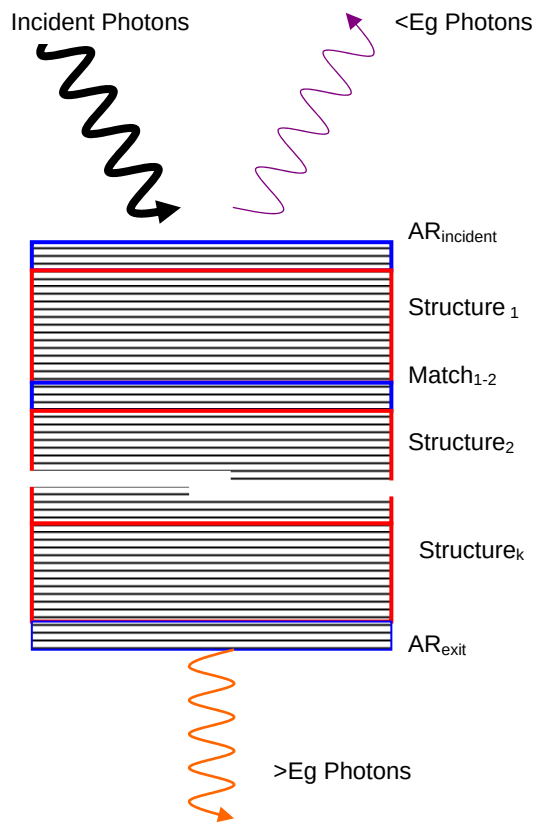

Explanation:

$AR_{incident}$ – refers to the structure that insures the photons pass into the subsequent structures to be 'processed' rather than reflect off the incident interface.

$Structure_1$, $Structure_2$, …$Structure_k$ – refers to the structures that provide the high reflection in the rejection band and corresponds to the spectral regions shown in the left figure.

$Match_{1-2}$ – refers to the structure that insures the photons pass into the subsequent structure.

AR_{exit} – refers to the structure that insures the photons pass out of the sequence of structures after 'processing' rather than reflect back into the sequence of structures at the exit interface.

Figure 3: Contribution of each component and physical arrangement of the filter

The structures shown in the development plan refer to a notation that is used to describe a general architecture for optical interference coatings (Reference (3)). The upper case letters, A and B, refer to the known low index material and the known high index material, respectively. The lower case letters, 'x' and 'y', refer to unknown materials that have a specified index of refraction for each architecture to maximize performance. In practice, a material with the

desired index of refraction is unavailable so an equivalent material is synthesized using alternating layers of materials with indices of refraction near the desired index of refraction.

Fabrication of the Optical Interference Coatings

To reach the potential performance offered by a given design of optical interference coatings, a fabrication process must create the optical interference coatings with the highest possible fidelity to the design. The intent of the initiatives described in this subsection is to increase the fidelity of the fabricated optical interference coatings and thus minimize the performance reduction of the fabricated coatings as compared to the design.

Fabrication of Tandem Filter that Enabled a New TPV Efficiency Record

In 2004, a tandem filter enabled a TPV module to achieve a new world record for efficiency. The tandem filter, KX12, was fabricated in December 2003 using the recently developed 767 design that was an evolution of the current design of the optical interference coatings as described earlier. As shown in Table 4, the tandem filter increased the efficiency 36.4% from the measured efficiency of the module with only a back surface reflector for spectral control. The measured, 22.1% efficiency represents a 10% increase over the previous world record of 20.0%. Moreover, the 10% increase was due solely to the tandem filter as the TPV cell performance was actually lower than TPV cell used for the 20% measurement. As shown in Table 4, the performance of the HEM7a TPV module (without the tandem filter) was higher than the performance of the HEM14a TPV module (without the tandem filter) used to achieve the 22% efficiency record.

However, the KX12 tandem filter was imbalanced with a low above band gap transmission as compared to the spectral efficiency. As a result, the tandem filter reduced the measured power density by 25.5%. Tandem filters with a better balance between the spectral efficiency and above band gap transmission have been fabricated. These filters have measured spectral efficiency that are 1-2% lower than KX12.

Table 4: Measured Performance of 0.60eV (nominal) Thermophotovoltaic Modules

Module / Filter	Spectral Control	Module		Tandem Filter	
		Efficiency* (%)	Power Density* (W/cm^2)	Spectral Efficiency (%)**	Above Band Gap Transmission (%)**
HEM7a	BSR only	17.3	0.520	—	—
HEM9a (w/ KU06)	Tandem Filter	20.0	0.456	72.5 / 69.1	77.3 / 77.9
	Δ	15.6%	(12.3%)	—	—
HEM14a	BSR only	16.2	0.490	—	—
HEM15a (w/ KX12)	Tandem Filter	22.1	0.365	77.9 / 75.7	72.6 / 72.9
	Δ	36.4%	(25.5%)	7.4%	(6.1%)

* Performance at reference conditions (~125F module temperature, ~1750F etched SiC radiator temperature (References (1, 2)),

** Adjusted Value / As-Measured Value, the two values of performance are listed for spectral efficiency and above band gap transmission due to the uncertainty associated with the optical characterization. See the text for a description of the difference between these values.

The HEM15a module failed just after sufficient data was gathered to ascertain performance at the reference conditions. To address this failure and a few others, several initiatives were begun to identify and address the cause(s) of the failures.

As will be seen throughout this document, two sets of results for each measurement are provided. The 'baseline' or 'as-measured' results represent the performance with only the Au reflectance correction (0.985) applied to the measured spectral reflection data. In addition to this correction, the 'adjusted' results represent the performance with a shift of the spectral reflection data so that the peaks reach about 99.99%. The need for the adjusted results will be discussed in a later section.

Fabrication of a Tandem Filter Set to Support First Small Array Test

The sustained fabrication of tandem filters described later yielded a subset of filters that were used for the first Small Array Test (SAT1). Of the 43 tandem filters fabricated to support these arrays, the 12 tandem filters with the highest above band gap transmission were selected for SAT1 to maximize the photon flux reaching each TPV cell and therefore maximize the power density achieved by the array. In addition, the selected tandem filters were placed on the array to minimize flux variation reaching the TPV cells connected in series and thus minimize current mismatch as shown in Figure 4. The TPV cells were connected in series vertically (relative to the sketch), and the series connection continued outside column of cells to outside column of cells and inside column of cells to inside column of cells. Later, however, an analysis of network efficiency showed that the overall variation in the above band gap transmission efficiency for all the tandem filters fabricated for the Small Array Tests would cause negligible network efficiency losses, and thus the selection of the tandem filters to minimize flux variation was unnecessary (Reference (4)).

Until assembly of this array, spectral efficiency dominated tandem filter development since spectral efficiency impacts the measured TPV efficiency of a module more than above band gap transmission. The selection of the tandem filters for the first array emphasizes the importance of both spectral efficiency and above band gap transmission.

80.8	82.0	81.0	80.2
80.6	81.4	80.9	80.3
81.0	81.2	81.0	80.2

(a) Above Band Gap Transmission of Each of the 12 Tandem Filters Used in SAT1

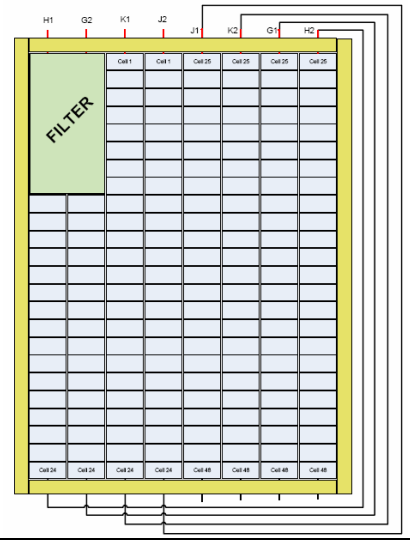

(b) General Arrangement of the Tandem Filters Relative to the TPV Cells

Figure 4: Above Band Gap Transmission of Tandem Filters Used in SAT1

Fabrication of Higher Performing Tandem Filters

Since January 2003, the spectral efficiency performance of both the 0.52eV and 0.60eV (nominal) tandem filters increased with several filters of both band gaps achieving both high spectral efficiency performance and at the same time high above band gap transmission performance. For tandem filters, high performance of one characteristic often occurs at the expensive of the other characteristic. Ideally, both performance characteristics should be high and thus balanced. Table 5 and Table 6 show comparisons of the best, measured performance between the tandem filters fabricated before January 2003 and the tandem filters fabricated after 2003.

Table 5: Comparison of Best-to-Best Tandem Filter for 0.52 eV Tandem Filters

		Current		Previous		
		adjusted	as-measured	adjusted	as-measured	Δ*(%)
Best	η (%)	83.7	82.3	78.9	72.8	6.1
Spectral	$T_{>Eg}$ (%)	80.5	80.9	72.8	73.5	
Efficiency	Edge (μm)	2.36	2.36	2.35	2.35	
	ID	KX34-2		KS106		
Best	η (%)	80.0	77.5	78.3	77.1	
Above Band	$T_{>Eg}$ (%)	82.0	82.6	81.6	82.2	0.5
Gap	Edge (μm)	2.42	2.42	2.39	2.39	
Transmission	ID	KX36-4		KU17		

* Percent change is based on the adjusted values.

Table 6: Comparison of Best-to-Best Tandem Filter for 0.60 eV (nominal) Tandem Filters

		Current		Previous		
		adjusted	as-measured	adjusted	as-measured	Δ*(%)
Best	η (%)	77.9	75.7	72.7	69.1	7.2
Spectral	$T_{>Eg}$ (%)	72.6	72.9	82.4	83.1	
Efficiency	Edge (μm)	2.01	2.01	2.09	2.09	
	ID	KX12		KU15		
Best	η (%)	77.2	74.7	72.7	69.1	
Above Band	$T_{>Eg}$ (%)	80.1	80.5	82.4	83.1	(2.8)
Gap	Edge (μm)	2.06	2.06	2.09	2.09	
Transmission	ID	KX27		KU15		

* Percent change is based on the adjusted values.

The best-to-best comparisons show that the measured, spectral efficiency performance of the tandem filter advanced 6-7%. With the same comparison, the above band gap transmission remained flat or decreased. As stated earlier, higher performance of one figure of merit can occur at the expense of the other figure of merit, and balanced performance is the most desirable. For the tandem filters listed in Table 6, for example, KX27 is the most balanced and thus most desirable filter as compared to KX12 and KU15. To be sure, high spectral efficiency at the expensive of above band gap transmission helps achieve new TPV efficiency records, but for any application of heat-to-electrical energy conversion, balanced tandem filters will be needed. In addition to balanced tandem filters, variations in filter performance from run-to-run, within a run, and within a filter need to be minimized as presented in the next few sections.

Fabrication of Three Classes of Tandem Filters

Three primary classes of tandem filters were developed and fabricated since January 2003. The 56L/84L[1] class and the 767 class of optical interference coatings represent an evolution of the optical interference coatings design prior to January 2003. The 767 class is the latest and last class to use the filter defined edge configuration and achieved the highest spectral efficiency and above band gap transmission performance. The G class design represents a completely different design approach and was the first and only design of the optical interference coatings for TPV energy conversion for the cell defined edge configuration that was described earlier.

Table 7 and Table 8 present comparisons between 56L/84L class and the 767 class of optical interference coatings for each TPV cell band gap. The results of the tandem filters fabricated for the Small Array Test are shown in a later section. Table 9 presents a comparison of Sb_2Se_3 based G class tandem filters and GaTe based G class tandem filters.

Table 7: Measured Performance Summary for 0.6 eV (nominal) Tandem Filters

Number of tandem filters		56L Class 14		767 Class 24	
		adjusted	as-measured	adjusted	as-measured
Edge Location (μm)	Mean	1.98	1.98	2.04	2.04
	Std Deviation	0.09	0.09	0.04	0.04
	Maximum	2.10	2.10	2.11	2.11
	Minimum	1.78	1.78	1.97	1.97
Spectral Efficiency (%)	Mean	71.5	67.3	75.1	72.6
	Std Deviation	5.5	4.6	2.3	3.0
	Maximum	77.2	72.3	77.9	77.6
	Minimum	58.6	58.0	68.8	67.2
Above Band Gap Transmission (%)	Mean	69.8	70.6	73.8	74.2
	Std Deviation	9.4	9.5	3.9	4.0
	Maximum	78.8	79.8	80.1	80.5
	Minimum	47.9	48.4	66.7	66.8
Below Band Gap Reflectance (%)	Mean	94.7	93.3	95.4	94.6
	Std Deviation	0.9	1.0	0.7	1.0
	Maximum	95.8	94.3	96.2	96.4
	Minimum	93.2	90.5	93.2	92.6

[1] The 56L/84L class represents two optical interference coatings designs: the 56L design has a 0.60eV (nominal) filter edge for 0.60eV TPV cells, and the 84L design has a 0.52eV filter edge for 0.52eV TPV cells. The 767 class also represents two different designs for optical interference coatings but use the same name. A 767 design was created for a 0.60ev (nominal) TPV cell as well as a 0.52eV TPV cell.

Table 8: Measured Performance Summary for 0.52 eV Filter Defined Edge, Tandem Filters

		84L Class		767 Class*	
Number of tandem filters		7		4	
		adjusted	as-measured	adjusted	as-measured
Edge Location (μm)	Mean	2.29	2.29	2.31	2.31
	Std Deviation	0.07	0.07	0.03	0.03
	Maximum	2.36	2.37	2.34	2.34
	Minimum	2.15	2.15	2.27	2.27
Spectral Efficiency (%)	Mean	80.3	77.5	82.8	80.9
	Std Deviation	2.2	2.2	1.2	2.4
	Maximum	82.4	80.8	83.7	82.9
	Minimum	75.9	74.2	81.2	77.8
Above Band Gap Transmission (%)	Mean	73.3	74.0	77.9	78.3
	Std Deviation	4.7	4.9	2.3	2.4
	Maximum	78.2	79.1	80.4	81.0
	Minimum	63.9	64.0	75.3	75.7
Below Band Gap Reflectance (%)	Mean	94.9	93.6	95.6	94.7
	Std Deviation	0.6	0.8	0.6	1.1
	Maximum	95.7	94.8	96.0	95.6
	Minimum	93.9	92.1	94.7	93.2

* Excludes the 0.52 eV tandem filters fabricated for the Small Array Test (SAT) shown in Table 11.

Table 9: Summary of Measured Performance of 0.60eV (nominal) Cell Defined Edge, Tandem Filters

		G Class (Sb_2Se_3)		G Class (GaTe)	
Number of tandem filters		6		27	
		adjusted	as-measured	adjusted	as-measured
Edge Location (μm)	Mean	2.08	2.08	2.13	2.13
	Std Deviation	0.08	0.08	0.05	0.05
	Maximum	2.12	2.12	2.26	2.26
	Minimum	1.93	1.93	2.05	2.06
Predicted TPV Efficiency* (%)	Mean	18.85	18.20	17.53	16.36
	Std Deviation	0.92	1.23	0.82	0.71
	Maximum	19.80	19.20	18.97	17.56
	Minimum	17.30	16.00	15.74	15.03
Predicted TPV Power* Density (W/cm^2)	Mean	0.414	0.419	0.421	0.425
	Std Deviation	0.059	0.056	0.024	0.022
	Maximum	0.456	0.458	0.445	0.448
	Minimum	0.304	0.313	0.361	0.370

* Predicted TPV efficiency and power density based measured performance of the tandem filters.

In general, the 767 class of tandem filter of each band gap have higher performance than the 56L/84L class of filters. Both the adjusted and the as-measured means were greater, and both the adjusted and the as-measured standard deviations[2] were lower for the 767 class. On the other hand, the maximum or best spectral efficiency or above band gap transmission are nearly the same for each class. Although the reason for this difference is uncertain, the maximum, as-measured value of the spectral efficiency for the 56L class was 7% lower than the value for the 767 class.

The fabricated, G class tandem filters using Sb_2Se_3 have about a 7% greater TPV efficiency than the fabricated, G class tandem filters using GaTe. The TPV power density, on the other hand, is slightly better for the GaTe based filters as compared to the Sb_2Se_3 filters. For comparable levels of optical interference coatings complexity, the Sb_2Se_3 based filters are expected to perform better because the Sb_2Se_3 has a greater index of refraction with comparable or lower levels of absorption. The difference in the TPV power density is likely due to the design used for the Sb_2Se_3 based filters which had a power density that was about 6% less than the power density for the more recent GaTe design. In other words, additional development would likely lead to a more power dense design for the Sb_2Se_3 based filters as compared to the GaTe based filters.

Comparison of the filter defined edge configuration and the cell defined edge configuration is possible but inappropriate since designs and associated fabrication were optimized differently for each configuration. Each configuration was optimized using different figures of merit. So to compare one to the other using one or the other figures of merits would only show that each configuration was more optimized to the given figure of merits than the other configuration, an obvious and therefore trivial conclusion. Moreover, to compare a cell defined edge configuration using spectral efficiency, the reflectance from the back surface reflector would need to be included since the design was optimized with the reflectance from the back surface reflector considered.

An appropriate and useful comparison between the filter defined edge configuration and the cell defined edge configuration is measured results from a TPV cell and filter module. Two such module tests have been completed with optimized tandem filters that used the cell defined edge configuration. Comparison between the results is difficult since one of these tests included only results at non-reference conditions and only results for a TPV cell and filter module (no results for the TPV cells only). As an extension of a previous table, Table 10 shows a comparison of measured results for TPV module at reference conditions (1750F radiator surface / 125F module).

[2] As a reminder, the standard deviation is the square root of the variation and as such has the same units as the mean values.

Table 10: Measured Performance of 0.60eV (nominal) Thermophotovoltaic Modules

Module (Filter)	Spectral Control	Module Efficiency* (%)	Power Density* (W/cm^2)	Tandem Filter Spectral Efficiency (%)**	Above Band Gap Transmission (%)**
HEM7a	BSR only	17.3	0.520	—	—
HEM9a (w/ KU06)	Tandem Filter	20.0	0.456	72.5 / 69.1	77.3 / 77.9
	Δ	15.6%	(12.3%)	—	—
HEM14a	BSR only	16.2	0.490	—	—
HEM15a (w/ KX12)	Tandem Filter	22.1	0.365	77.9 / 75.7	72.6 / 72.9
	Δ	36.4%	(25.5%)	—	—
				Predicted TPV Efficiency* (%)	Predicted Power Density* (W/cm^2)
HEM29a	BSR only	15.1	0.543	—	—
HEM31a (w/ KD32)	Tandem Filter	20.0	0.450	19.6 / 18.7	0.456 / 0.458
	Δ	32.5%	(17.1%)		

* Performance at reference conditions (~125F module temperature, ~1750F etched SiC radiator temperature)
** The two values of performance are listed for spectral efficiency and above band gap transmission due to the uncertainty associated with the optical characterization. This uncertainty will be described later in this report.

As expected, the tandem filter with the cell defined edge configuration (KD32) improved efficiency performance and decreased power density performance of the TPV module HEM29a. Specifically, from Table 10, the efficiency increased 32.5% with the addition of the tandem filter to create module HEM31a as compared to the increase of 36.4% with the addition of the tandem filter to create module HEM15a that used a tandem filter with the filter defined edge configuration. The 10% decrease in measured efficiency for the HEM31a module as compared to the HEM15a module is due to the lower performing TPV cell and the lower performing tandem filter used for HEM31a. Comparing the TPV cells without the tandem filter, HEM29a had an approximately 10% lower performance than HEM14a (15.2% as compared to 16.2%). In addition, the spectral efficiency of the tandem filter used to create HEM31 was lower than the tandem filter used to create HEM14a based roughly on the percentage improvement over the performance without the tandem filter (32.5% as compared to 36.4%).

Comparison of the above band gap transmission efficiency of the of the tandem filter used to create HEM31 with the tandem filter used to create HEM14a is problematic since the measured decrease (25.5%) in power density is anomalous. A better comparison of the power density decrement for the tandem filter addition can be made between modules HEM9a (12.3%) and HEM31a (17.1%). Again with this comparison, the tandem filter, KD32, used in module HEM31 had a lower performance for above band gap transmission.

The tandem filter, KD32, used to create HEM31a was fabricated early in the development of the cell defined edge configuration and additional development is expected to improve the performance of tandem filters with this configuration.

Development of an Approach to Increase Fabrication Fidelity

To increase fabrication fidelity, online monitoring of the spectral transmittance or reflectance of the evolving optical properties of optical interference coatings as each layer is deposited in a physical vapor deposition process was proposed as a powerful tool to assure that the deposited material has the intended thicknesses and optical properties. The primary interest in seeking online monitoring of evolving optical properties would be to better understand the performance of the fabrication system and identify any abrupt changes in the performance of the fabrication system (Reference (5)). For example, is the index of refraction of one the materials in the optical interference coatings different than with the previous fabrication run or drifting during the run? For now, single layer coatings of each material are deposited using the actual physical vapor deposition system to represent the optical properties of the materials within optical interference coatings. However, the actual optical properties and thicknesses of the materials deposited during a given fabrication run are uncertain.

Currently, the fabrication vendor, Rugate Technologies, Inc. has successfully fabricated the optical interference coatings for a tandem filter by monitoring deposition rate and layer thickness using piezoelectric microbalances. This monitoring infers the deposition rate and layer thicknesses based on the changing vibratory frequency of the microbalances as they accumulate material. Online monitoring of the spectral transmittance or reflectance would measure the thickness and optical properties (index of refraction and absorption) of each layer by inference using characteristics of the spectral transmittance or reflectance. This additional online monitoring would complement the existing online monitoring of the microbalances. Rugate Technologies, Inc. has sought online monitoring of the evolving optical properties over the last few years but to date has not successfully implemented a system.

Fidelity of the fabricated, aggregate optical interference coatings relative to the design of the optical interference coatings is difficult to quantify, and hence the interest in monitoring of the spectral transmittance or reflectance of the evolving optical properties. Comparing the measured, overall performance of the fabricated tandem filters to the associated design performance is straightforward and useful, but understanding the inevitable differences requires knowledgeable inferences of the shape and magnitude of the spectral reflectance.

For example, a comparison of the ‘as designed’ and ‘as fabricated’ performance of a 0.60eV (nominal) tandem filter is show in Figure 1. Two different design performances are show in the figure, one with absorbed water in the exterior layer of YF_3 and one without absorbed water in the layer. As shown in the figure, the design performance with the absorbed water has two dips in the reflectance at about 3µm. This example shows an extreme but well known feature of the tandem filters, they can absorb moisture when exposed the atmosphere of the fabrication room. Other features that appear in fabricated tandem filters are not necessary well understood or as easily identified.

Performance differences exist between fabricated coatings and the design of the coatings because layer thicknesses differ and the properties of the deposited materials differ. Online

monitoring of optical properties may help determine systematic or sporadic differences in specific layer thicknesses or the properties of a specific, deposited material that the comparison of the fabricated, aggregate optical interference coatings relative to the design cannot provide.

Implementation of Sustained Fabrication of Tandem Filters

For the first time several sets of multiple filter fabrication runs were completed to rapidly fabricate tandem filters for the small array test (SAT). These sets of fabrication runs provided an indication of fabrication process variation within and between runs. In general, as is appropriate for a development program, each fabrication run for the optical interference coatings was somewhat unique in that a slightly different design was attempted or a fabrication change was attempted to learn the influence of the change. Therefore assessing the variation in the fabrication process is difficult.

Eleven fabrication runs with four wafers in each run were completed. The measured results of these runs are shown in Table 11. The optical interference coatings deposited during the physical vapor deposition runs were for 0.52eV TPV cells. The optical interference coatings deposited during these runs were intentionally altered to shift the edge between the low reflectance to high reflectance to a higher wavelength.

Table 11: Measured Performance Summary for 0.52 eV Filter Defined Edge, Tandem Filters Fabricated for the Small Array Test (SAT)

Number of tandem filters		767 (SAT) Class 43*	
		adjusted	as-measured
Edge Location (µm)	Mean	2.39	2.39
	Std Deviation	0.07	0.07
	Maximum	2.53	2.53
	Minimum	2.25	2.25
Spectral Efficiency (%)	Mean	80.0	78.9
	Std Deviation	3.2	3.2
	Maximum	83.8	83.8
	Minimum	71.9	70.1
Above Band Gap Transmission (%)	Mean	77.5	77.9
	Std Deviation	4.1	4.2
	Maximum	82.0	82.6
	Minimum	66.1	66.0
Below Band Gap Reflectance (%)	Mean	94.4	93.9
	Std Deviation	1.3	1.4
	Maximum	96.0	95.9
	Minimum	90.9	89.8

* During characterization, one of the forty four tandem filters was dropped causing the tandem filters to break and precluding any measurements.

From the results shown in Table 11, the fabrication runs achieved a mean spectral efficiency of 80.0% with a standard deviation of 3.2% and a mean above band gap transmission of 77.5% with a standard deviation of 4.1% using the adjusted values.

As expected, with the shifted edge, the mean spectral efficiency decreased to 80.0% for the 0.52eV, 767 tandem filters in Table 11 as compared to the 82.8% efficiency for the 0.52eV, 767 tandem filters in Table 8. Interestingly, the mean above band gap transmission remained nearly constant at 77.5% for the tandem filters in Table 11 in comparison to the 77.9% for the tandem filters in Table 8. The mean edge for the tandem filters in Table 11 was 2.39 in comparison to 2.31 for the mean edge of the tandem filters in Table 8. Finally, these conclusions may be dependent on the size of the population between the two sets of tandem filters. The tandem filter set described in Table 11 contains 43 filters; whereas, the tandem filter set described in Table 8 contains only 4 filters.

In general, any fabrication variation is undesirable. To further assess the sources of the variation, a two-way analysis of variance (ANOVA) of the measured results was completed[3]. Table 12 and Table 13 contain the results of the ANOVA analysis. Table 12 presents the results of the hypothesis tests on each of the responses, namely edge location, spectral efficiency, above band gap transmission, and below band gap reflectance. Two sources of variation are modeled, run-to-run (labeled as 'Run') and within run (labeled as 'Wafer'). The hypotheses are that neither of the sources have any effect on the responses. The degrees of freedom (labeled 'DF') and the sum of the squares are calculations step typically presented along with test statistic (labeled 'F Ratio') as the critical value used to determine the level of significance. This level of significance is indicated by the P-value (labeled 'Prob>F'). The P-value is the probability that the hypothesis is true. Taking the first response in Table 12, for example, the probability of the run-to-run source ('Run') having no effect on the response is low (<0.0001). In other words, the probability that the hypothesis is true is low, and therefore, the run-to-run source definitely does have an effect the response. In contrast the probability of the within run source ('Wafer') having no effect on the response is high (0.9811). Again, the probability that the hypothesis is true is high, and therefore, the within run source definitely has little effect the response.

Moreover, the total variance can be separated into a component due to run-to-run variability and a component due to residual variability within runs as shown in Table 13. In this table the run-to-run component of variability is grouped with the random variability and compared to the residual component of variability which in this case is the within run variability. Taking the second response in the table, for example, 89% of the variation in the spectral efficiency (adjusted) is due to run-to-run and random variation with only the remaining 11% due to within run variation.

Figure 5 contains a plot of the individual responses for each run to check that no bias in the results that would violate an assumption in the ANOVA analysis. As shown in the figure, no bias is evident.

[3] Dan Eno performed the two-way analysis of variance (ANOVA).

Table 12: Two-Way Analysis Of Variance (ANOVA) of Multiple Tandem Filter Fabrication Runs

Adjusted Results

Response: Edge Location Effect Tests

Source	DF	Sum of Squares	F Ratio	Prob > F
Run	10	0.20351851	37.5401	<.0001
Wafer	3	0.00009520	0.0585	0.9811

Response: Spectral Efficiency Effect Tests

Source	DF	Sum of Squares	F Ratio	Prob > F
Run	10	0.03870631	29.9516	<.0001
Wafer	3	0.00012085	0.3117	0.8167

Response: Above Band Gap Transmission Effect Tests

Source	DF	Sum of Squares	F Ratio	Prob > F
Run	10	0.06828932	55.2689	<.0001
Wafer	3	0.00040323	1.0878	0.3699

Response: Below Band Gap Reflectance Effect Tests

Source	DF	Sum of Squares	F Ratio	Prob > F
Run	10	0.00682278	28.7767	<.0001
Wafer	3	0.00002143	0.3012	0.8242

As-Measured Results

Response: Edge Location Effect Tests

Source	DF	Sum of Squares	F Ratio	Prob > F
Run	10	0.20311713	37.6792	<.0001
Wafer	3	0.00009624	0.0595	0.9806

Response: Spectral Efficiency Effect Tests

Source	DF	Sum of Squares	F Ratio	Prob > F
Run	10	0.03631375	17.2402	<.0001
Wafer	3	0.00010852	0.1717	0.9146

Response: Above Band Gap Transmission Effect Tests

Source	DF	Sum of Squares	F Ratio	Prob > F
Run	10	0.07063740	55.1983	<.0001
Wafer	3	0.00041128	1.0713	0.3766

Response: Below Band Gap Reflectance Effect Tests

Source	DF	Sum of Squares	F Ratio	Prob > F
Run	10	0.00728911	18.1136	<.0001
Wafer	3	0.00002492	0.2065	0.8911

Table 13: Estimated Components of the Variation

Adjusted Results

Response: Edge Location Variance Component Estimates

Component	Var Comp Est	Percent of Total
Run&Random	0.005089	91.148
Residual	0.000494	8.852
Total	0.005584	100.000

These estimates based on equating Mean Squares to Expected Value.

Response: Spectral Efficiency Variance Component Estimates

Component	Var Comp Est	Percent of Total
Run&Random	0.000964	88.858
Residual	0.000121	11.142
Total	0.001085	100.000

These estimates based on equating Mean Squares to Expected Value.

Response: Above Band Gap Transmission Variance Component Estimates

Component	Var Comp Est	Percent of Total
Run&Random	0.001715	93.228
Residual	0.000125	6.772
Total	0.00184	100.000

These estimates based on equating Mean Squares to Expected Value.

Response: Below Band Gap Reflectance Variance Component Estimates

Component	Var Comp Est	Percent of Total
Run&Random	0.00017	88.455
Residual	0.000022	11.545
Total	0.000192	100.000

These estimates based on equating Mean Squares to Expected Value.

As-Measured Results

Response: Edge Location Variance Component Estimates

Component	Var Comp Est	Percent of Total
Run&Random	0.00508	91.178
Residual	0.000492	8.822
Total	0.005572	100.000

These estimates based on equating Mean Squares to Expected Value.

Response: Spectral Efficiency Variance Component Estimates

Component	Var Comp Est	Percent of Total
Run&Random	0.000884	81.984
Residual	0.000194	18.016
Total	0.001078	100.000

These estimates based on equating Mean Squares to Expected Value.

Response: Above Band Gap Transmission Variance Component Estimates

Component	Var Comp Est	Percent of Total
Run&Random	0.001774	93.229
Residual	0.000129	6.771
Total	0.001903	100.000

These estimates based on equating Mean Squares to Expected Value.

Response: Below Band Gap Reflectance Variance Component Estimates

Component	Var Comp Est	Percent of Total
Run&Random	0.000178	82.691
Residual	0.000037	17.309
Total	0.000215	100.000

These estimates based on equating Mean Squares to Expected Value.

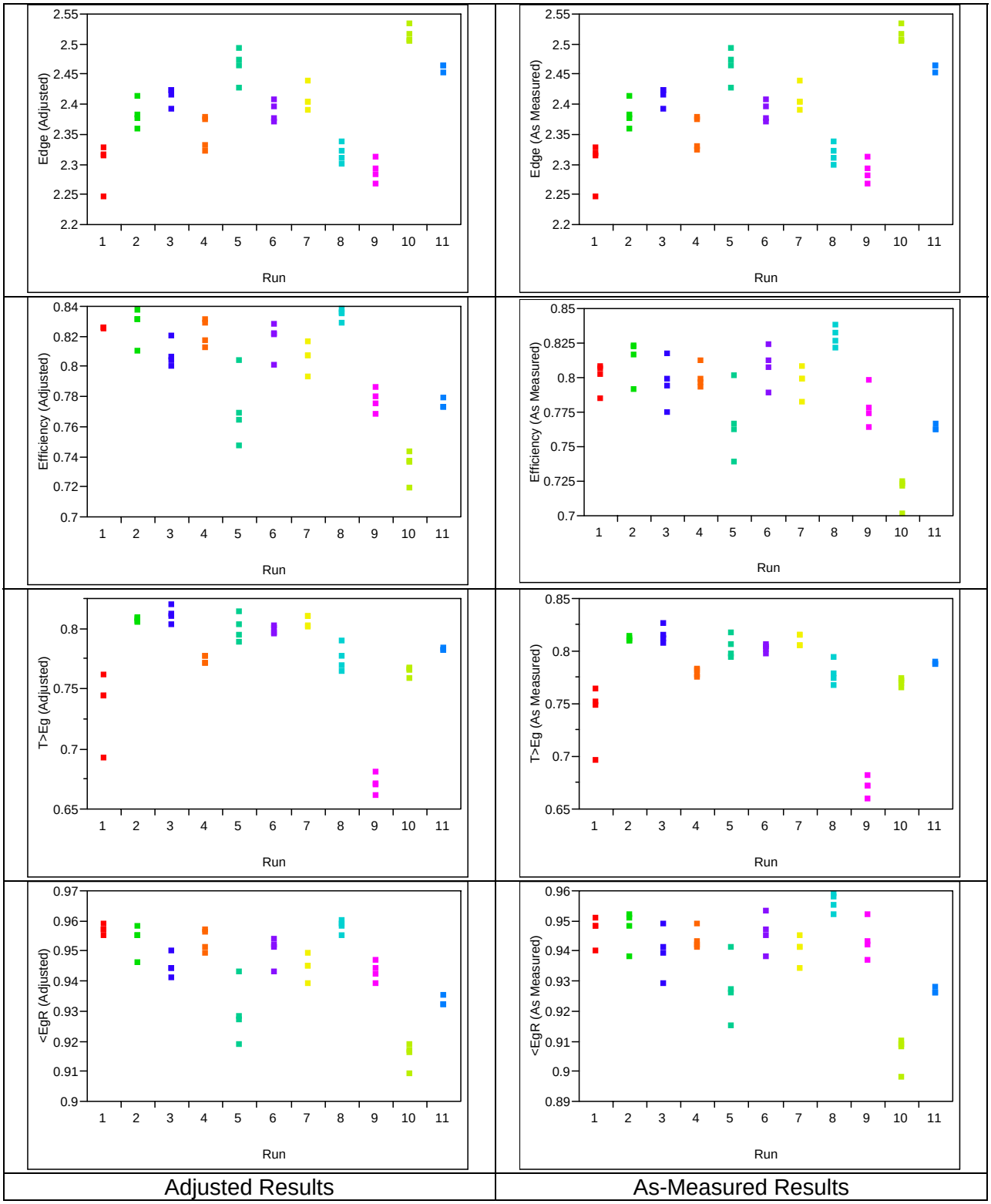

Figure 5: Individual Responses for Each Run to Check Run Bias

The two-way ANOVA of the 0.52eV tandem filter fabrication runs showed that the run-to-run variation was statistically significant while the within run variation was statistically insignificant. Therefore, the majority of the variation in the various figures of merit (referred to as the responses) is due to run-to-run variation. In all cases, the within run variation was found to be not statistically significant. Furthermore, in all cases, the run-to-run and the random variation accounted for more than 80% of the variation.

Across a wafer variation presents another source of variation in addition to the run-to-run and the within run variation and was addressed as described in the next section.

Modification of Fabrication System to Improve Deposition Uniformity

With the fabrication of 3 inch diameter tandem filters, the across wafer standard deviation of the edge location was measured and found to be 8-10%. To reduce the across wafer variation, Rugate Technologies, Inc. developed a deposition uniformity mask for the vacuum chambers used in the physical vapor deposition of the optical interference coatings. The modification reduced across wafer variation considerably so that the standard deviation for 3 inch diameter wafers was measured to be less than 1.5%. The standard deviation across a 2 inch diameter wafer was measured to be less than 1.0% with the modification.

To confirm these measurements, the across wafer variation was measured independently and differently. Rugate Technologies, Inc. used three statistics, edge location, a transmittance statistic, and a reflectance statistic, to assess variation. KAPL measured two locations along the diameter of two tandem filters that were fabricated subsequent to the uniformity modification to the vacuum chambers. Edge location, predicted TPV efficiency, and predicted TPV power density efficiency, were the statistics used to characterize the measured spectral and direction reflectance data. Figure 6 and Figure 7 present the results of the across wafer uniformity characterization. From the results shown in the figures, the across wafer standard deviations for 2 inch diameter tandem filters were less than 0.5%

KD32 Location	η_{TPV}	PD_{TPV}	Edge
A	18.68	0.459	2.13
B	18.81	0.458	2.12
Mean	18.75	0.459	2.125
Std.Dev.	0.092	0.001	0.007
A adj	19.71	0.456	2.12
B adj	19.36	0.457	2.12
Mean	19.54	0.457	2.12
Std.Dev.	0.247	0.001	n/a

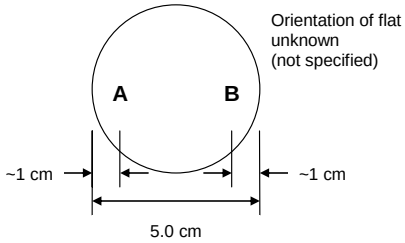

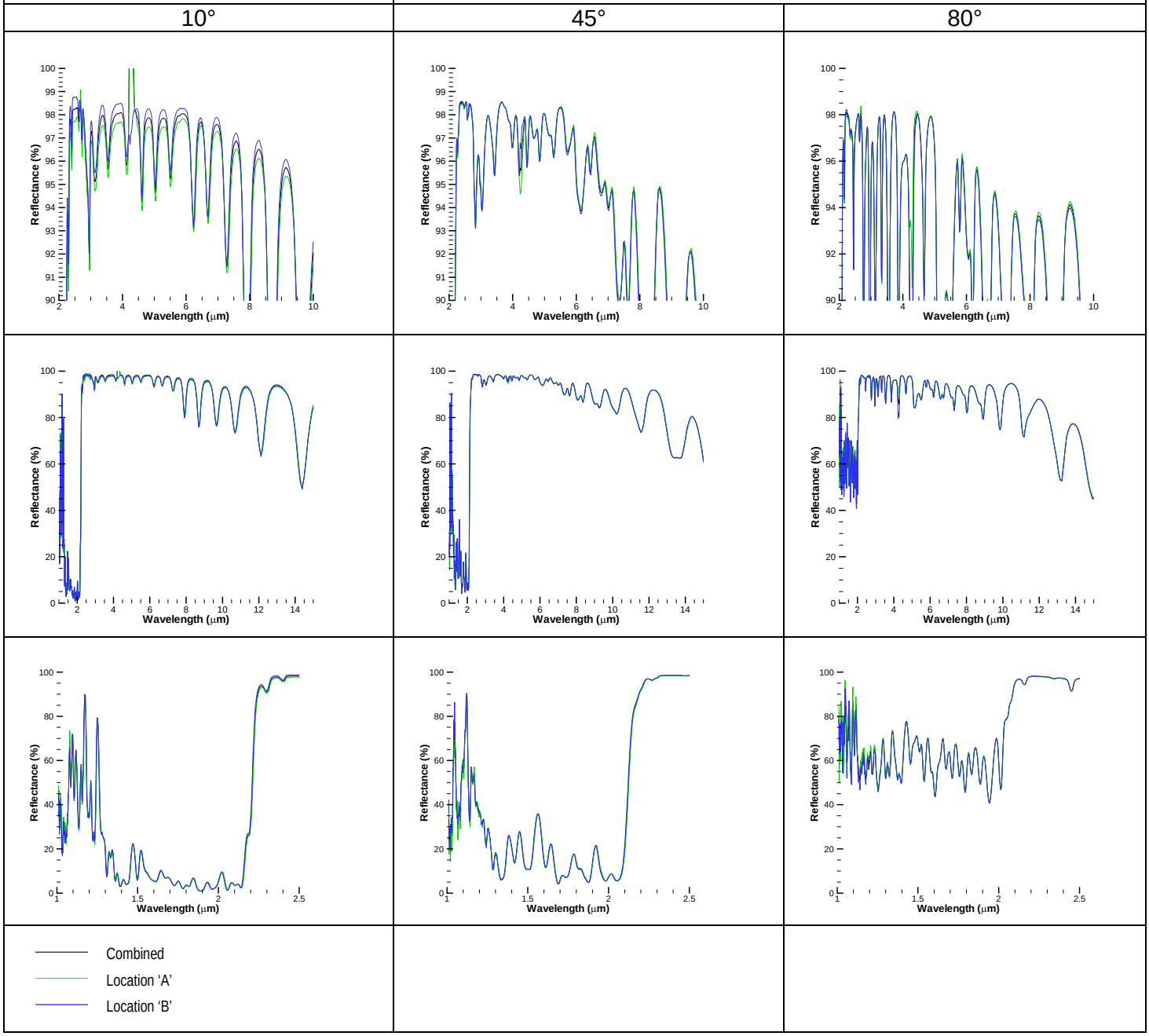

Figure 6: Across Wafer Uniformity for Tandem Filter, KD32

KD34 Location	η_{TPV}	PD_{TPV}	Edge
A	19.77	0.456	2.12
B	19.32	0.455	2.13
Mean	19.55	0.456	2.125
Std.Dev.	0.318	0.001	0.007
A adj	19.44	0.452	2.12
B adj	18.97	0.453	2.12
Mean	19.21	0.453	2.12
Std.Dev.	0.332	0.001	n/a

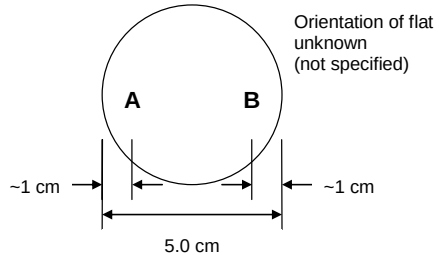

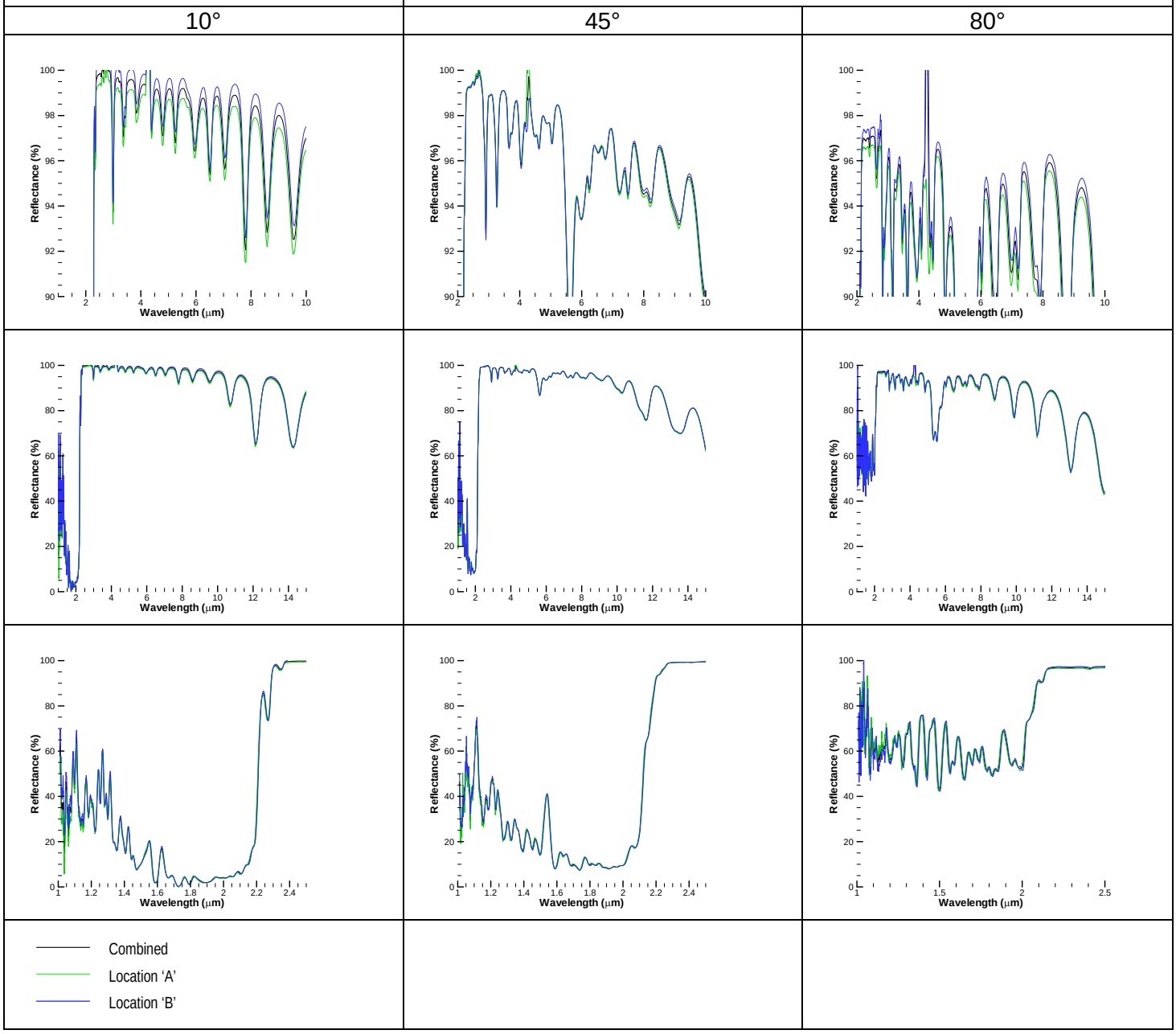

Figure 7: Across Wafer Uniformity for Tandem Filter, KD34

Modification of Fabrication System Cooling

Several modifications to the cooling loops in the physical vapor deposition system were completed to reduce the temperature difference between the microbalances and the platen from about 86F (30C) to about 39F (4C). The platen is a fixture that supports the substrate(s) (wafer(s)) during deposition of the coatings. Since the platen and the substrate(s) are in contact, the temperature of the substrate(s) is essentially the same temperature as the platen. The temperature difference between the microbalances and the platen was discovered as the result of a concerted effort to instrument the physical vapor deposition systems in order to improve the performance.

Microbalances are used to control the fabrication process by measuring the weight of the deposited materials. For accuracy, the microbalances should be at the same temperature as the substrate(s) being coated. Therefore, since the substrates are mounted on the platen, the microbalances and the platen should be at the same temperature. The remaining temperature difference between microbalance and the platen (and other factors) is accommodated with tooling factors that are set based on measured, single layer deposition runs.

Implementation of Source Material Conditioning Procedures

Conditioning of source material was identified as a potential significant, yet previously unknown cause of variation in the fabrication process. In 2003, it was discovered that the one of the source materials as received from the supplier was visually different from the remaining source material after a fabrication run. A year earlier, a single layer sample of this source was created for characterizing the as-deposited index of refraction, absorption, and layer thickness using spectroscopic ellipsometry. The results suggested that the absorption was much greater than expected. This result remained unresolved until Rugate Technologies, Inc., surmised that the as-received source material may be rich in one of the elements on the surface of the material base on observations of the as-received source material. Therefore, during evaporation and subsequent deposition on the wafer, the source material evaporated preferentially causing the deposited layer to be an elemental and molecular mixture rather than just the molecule desired. The existence of the elemental material in the layer increased the absorption. The solution, common to physical vapor deposition fabrication, was to condition the source material prior to using the material to fabricate optical interference coatings. The conditioning was accomplished by placing the source material into a vacuum oven and heating the material to a sufficient temperature to evaporate any surface elements while minimizing the evaporation of the desired molecular material. After implementation of the source conditioning step, another single layer sample of the source material was created for characterization. Using the same vendor and the same characterization technique, this sample showed the expected, low level of absorption. Conditioning of source material prior to deposition contributed to the decrease in fabrication variation and highlighted the need to continually watch the optical properties of the deposited materials.

Implementation of an Alternative Technique for Evaporation of Source Materials

Radiative evaporation of the GaTe was attempted and found to be the key to successfully evaporating GaTe and thus fabricating GaTe based tandem filters. Resistive heating evaporation and electron beam evaporation were attempted first for GaTe as both are currently used for the fabrication of the tandem filters. However, both evaporation techniques resulted in dissociation of GaTe and preferential evaporation of Te causing unacceptable optical absorption in the resulting evaporated material. Although no measurement of the resulting film to confirm the existence of Te was performed (due to work backlog of required characterization equipment), this conclusion is based on two facts. First, the vapor pressure of Ga is too low for evaporation of the disassociated Ga to occur, and second contaminate variations in the source material based vendor characterization did not correlate with the absorption in the various batches of the evaporated material.

Radiative evaporation, moreover, may be useful for the other materials, especially Sb_2Se_3. An alternative evaporation technique had been sought for the Sb_2Se_3 source material to enhance performance and reduce fabrication run time. The performance improvement would likely be small, since the fabricated tandem filters using resistive heating evaporation for the Sb_2Se_3 source material already have achieved the highest spectral efficiency to date and match the design or predicted values well. However, the fabrication run time currently is 12-14 hours and could be reduced by 20-25% if an alternative to resistive heating evaporation could be used. The decrease in the fabrication run time could reduce the cost of the process, reduce the risk of malfunction during a run, or allow even more complex (more layers) designs to be fabricated.

Electron beam evaporation was studied as an alternative to resistive heating evaporation that is currently used for the Sb_2Se_3 source material. Electron beam evaporation is generally preferable to resistive heating evaporation, since electron beam evaporation allows faster deposition on/off response and avoids the interaction of the source material and the crucible material (Reference (6)). In the current fabrication process, YF_3 is evaporated using electron beam evaporation. In the end, the capacity of the particular equipment used was postulated to be too great for the Sb_2Se_3 source materials. Evaporation of the Sb_2Se_3 in particular requires lower electron beam energy than the system could reliably deliver. In other words the controllability of the electron beam energy was insufficient at the levels that are required for the material.

Radiative evaporation development of Sb_2Se_3 was begun by Rugate Technologies, Inc., but development was halted with the termination of the program.

Optimization of Substrate Temperature and Deposition Rate

Substrate temperature and deposition rate were identified as the most likely variables to impact the run-to-run variability and the optical properties of the deposited materials. Therefore, to identify the optimum substrate temperature and deposition rate for each material, the four corner plus center experimental design show in Table 14 was developed and had begun to be implemented before termination of the program. This experimental design presumes that other variables such as the operator, chamber, humidity, and so on can be controlled (that is held constant).

Table 14: Run Numbers for the Experimental Design of Selected Fabrication Parameters

Evaporation Technique	Deposition Rate	Substrate Temperature					
		Low		Midway		High	
Resistive	Low	1	2			3	4
Electron		5	6			7	8
Resistive	Midway			9	10		
Electron				11	12		
Resistive	High	13	14			15	16
Electron		17	18			19	20
Run order: 12, 1, 13, 8, 7, 11, 10, 16, 14, 3, 9, 19, 6, 4, 18, 15, 20, 17, 5, 2 Levels: Substrate Temperature, 176, 320, 464F (80, 160, 240C), Deposition Rate, 8, 15, 25 Å/second							

Only the runs for resistive heating of GaTe were completed. The results showed unacceptable absorption occurred for all combinations of the independent variable. The absorption was postulated to be the result of dissociation and the subsequent preferential evaporation of Te. The runs for the electron beam evaporation of GaTe were begun but were soon halted due to unacceptable absorption. In the end a third method (radiative, see previous discussion) of evaporation was attempted for GaTe and found to be satisfactory. Optimization of the substrate temperature and deposition rate for GaTe using radiative evaporation remains incomplete as well as optimization for the other materials used in the optical interference coatings for the TPV tandem filters.

Enhancement of Fabrication Operating Procedures

To continue to enhance run-to-run consistency, the operating procedures for the fabrication system were continually assessed and modified as appropriate. Two issues were identified just before the termination and were intended to be addressed through operating procedure changes.

The first issue is potential cross contamination of source material during the setup for a fabrication run. Currently, the operators use a single pair of gloves to replenish all source materials to be used during the run. It was observed that the gloves become dirty and therefore could transfer one source material into another source during replenishment and thus contaminate the source material. Potential operational changes would be to re-glove before handling each source material or clean gloved hands after handling each source material.

The second issue is potential inconsistencies in the evaporative plume resulting from the application of clean foil to the shutter after removal of the coated foil from the previous run during setup for a fabrication run. Inconsistent application of the foil could cause subtle changes in the shape of the evaporative plume reaching the substrates and changes to the evaporate plume could change the properties and the thicknesses of the deposited materials. To address this issue, a change to shutter and shutter support mechanisms to facilitate repeatable installation and removal of foil may be required.

Material Development for Optical Interference Coatings

The focus of the material development initiatives was the temperature stability of the materials used in the optical interference coatings and hence the temperature stability of the TPV tandem filters. These initiatives involved characterizing the temperature stability, both the instantaneous transformation temperature and the time-at-temperature stability, of the materials used in the existing optical interference coatings. More importantly, to increase the temperature stability of the TPV tandem filters, an initiative was begun to identify and develop an alternate, high index material, as the high index material was the limiting material in the existing optical interference coatings. The temperature stability of the tandem filters has been recognized as a significant implementation issue. The temperature stability of the tandem filter and thus the TPV module is one of many characteristics that determine the resiliency of an energy conversion system and hence the level of engineered protection system required to meet a given application.

Identification of an Alternate, High Index Material for the Optical Interference Coatings

Hassan Ehsani identified GaTe as potential alternative, high index material as a result of searching and evaluating numerous other materials. Then, Rugate Technologies, Inc. was asked to develop the ability to use physical vapor deposition in the fabrication of optical interference coatings for a tandem filter using GaTe as the high index material. After some difficulty, radiative evaporation was identified as the key to allow fabrication of the optical interference coatings using GaTe. Subsequently, numerous tandem filters were fabricated with GaTe, and two TPV modules were assembled and tested using a GaTe based filter. In addition, the instantaneous transformation temperature of GaTe was characterized, and time at temperature testing of GaTe based tandem filters was completed as described in the following two sections.

Characterization of the Instantaneous Transformation Temperature of All the Materials Used in the Optical Interference Coatings

An x-ray diffraction system with a heated sample stage was identified and used to assess the ‘instantaneous’ amorphous-to-crystalline transformation temperature. For some materials, transformation from an amorphous material to a crystalline material results in undesirable optical properties, namely higher optical absorption. For the first time, a characterization technique (x-ray diffraction) was used to assess the transformation temperature of representative samples of the materials used in the optical interference coatings for the tandem filters.

Single layer samples of each the materials used in the optical interference coatings on the tandem filters were deposited by Rugate Technologies, Inc. on glass (amorphous) substrates. Rugate Technologies, Inc. used the same physical vapor deposition systems and procedures to create the single layer samples as representative samples of the each material. As shown in Figure 8, the samples were heated from room temperature in steps and an X-Ray diffraction scan was completed at each step. The temperature at which sufficient crystallization occurred to be detected by the x-ray diffraction data was defined as the instantaneous transformation temperature. Table 15 contains a listing of the resulting instantaneous transformation temperatures for each tested material.

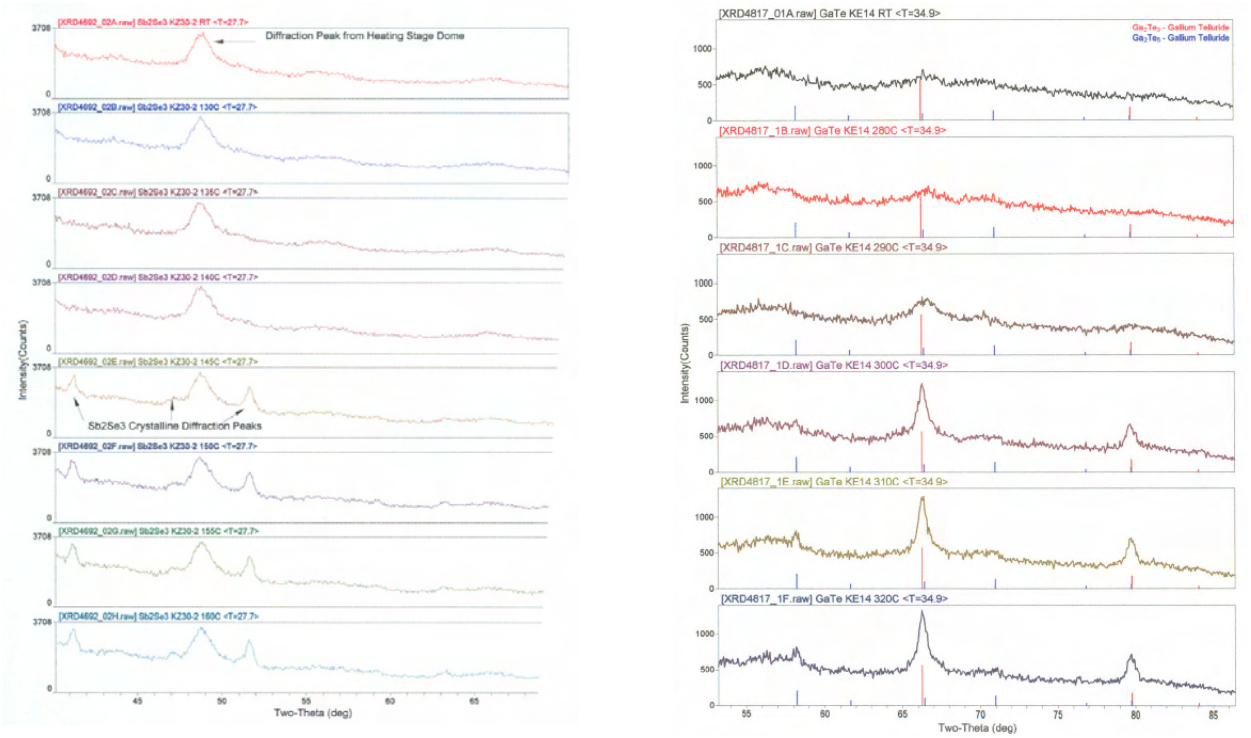

Sb_2Se_3 GaTe

Figure 8: Series of X-Ray Diffraction Scans of Sb_2Se_3 and GaTe at Various Temperatures Beginning at Room Temperature and Increasing Until Crystallization Occurred

Table 15: Estimated Instantaneous Transformation Temperatures for Various Materials

Material	Estimated Instantaneous Transformation Temperature
Sb_2Sb_3	284-250F (140-145C)
YF_3	518-536F (270-280C)
Sb_2S_3	482-500F (250-260C)
GaTe	554-572F (290-300C)

The transformation temperature for Sb_2Se_3 was confirmed to be 284-250F (140-145C) as had been assumed in the past. As a result, for Sb_2Se_3 based tandem filters, the Sb_2Se_3 is the limiting material, as expected. For GaTe based tandem filters, however, the GaTe may not be the limiting material as the transformation temperature for YF_3 is lower. In practice, the instantaneous transformation temperature does not necessarily define the operating conditions for a given material. Rather, the time at temperature before a sufficient percentage of a material transforms to cause failure of the material to maintain the required optical characteristics is crucial, as presented in the next section.

Characterization of the Time-at-Temperature Capability of the Sb_2Se_3 and GaTe Based Tandem Filters

For the first time, time-at-temperature stability was assessed for representative samples of tandem filters. The power density of a TPV energy conversion system directly correlates with the above band gap, spectral transmittance of a front surface tandem filter. As a result, any decrease in the transmittance of the tandem filter will result in a corresponding decrease in the power output and efficiency of a TPV energy conversion system.

The temperature stability of the Sb_2Se_3 based tandem filters has long been a concern. The key questions relative to this temperature stability are: (1) at what temperature would the TPV cell and filter need to be kept in order to maintain the properties of the Sb_2Se_3 based tandem filter over the required life of the system, and (2) how fast and how much would the performance of the Sb_2Se_3 based tandem filter degrade if the operating temperature was exceeded due to a coolant transient? The time-at-temperature testing presented in this section began to address these questions, but additional testing will be required to completely answer the questions.

Samples from tandem filters were placed in a vacuum oven at a specified temperature based on the transition temperature of each material used in the optical interference coatings for the tandem filters from the testing described in the previous section. The samples were removed periodically depending on the temperature for optical characterization using the FT-IR spectrometer as listed in Table 16. Samples were submitted to the highest temperatures first to limit initial testing time and to insure that changes in the optical properties of the filter could be characterized.

Table 16: Sb_2Se_3 Temperature Stability Test Matrix

Temperature		Time-at-Temperature for Each Characterization (Hours)					
(°C)	(°F)	1	2-10	11-1000		>1000	
		Sb_2S_3 based tandem filter samples					
80	176			337	505	1150	
100	212		8	330	624	1103	
110	230	1	9				
120	248	1	8				
130	266	1	9				
140	284	1					
150	302	1					
		GaTe based tandem filter samples					
150	302			256	880	1135	1583

The spectral transmittance at near normal incident angle at the temperatures and for the times show in Table 16 is presented in Figure 9, Figure 10, Figure 11, Figure 12, Figure 13, Figure 14, and Figure 15 for the Sb_2Se_3 based tandem filters. The spectral transmittance at a 10° incident angle at the temperatures and for the times shown in Table 16 is presented in Figure 16 for the GaTe based tandem filters.

For the samples from the GaTe based tandem filters, the spectral transmittance was measured at a 10° incident angle instead of a near normal incident angle. The reason for this difference is that concerns about near normal incident angle measurements for spectral transmittance using the FT-IR spectrometer emerged after the time-at-temperature testing of the Sb_2Se_3 based tandem filters had begun. As discussed earlier, the accuracy of the magnitude of the transmittance measurement at a near normal incident angle for the FT-IR spectrometer is uncertain. The precision, on the other hand, is sufficient to allow relative comparisons of measurements as has been done for the Sb_2Se_3 based tandem filters. To remove these concerns with the latest testing, the spectral transmittance at a 10° incident angle was used to characterize the samples from the GaTe based tandem filters.

When duplicate data sets were taken, error bars that represent the 95% confidence interval using a pooled value of the variance were plotted to indicate measurement variability.

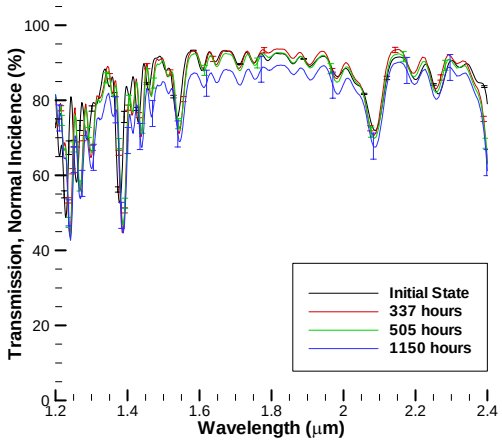

Filter ID: KX34-1

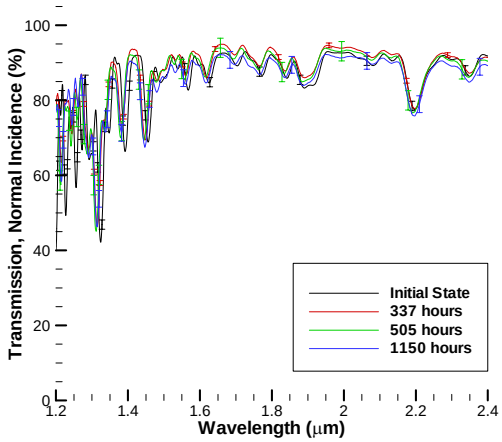

Filter ID: KX42-3

Figure 9: Sb_2Se_3 Based Tandem Filters Tested at a Temperature of 176F (80C)

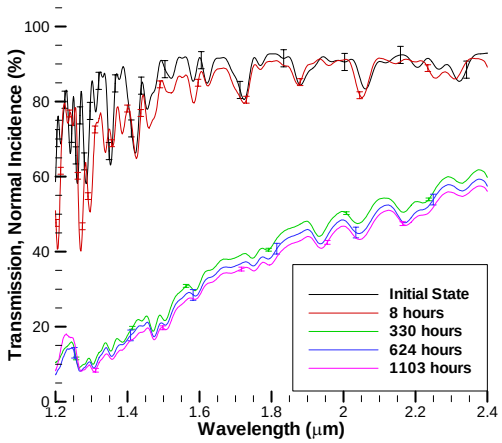

Filter ID: KX44-2a

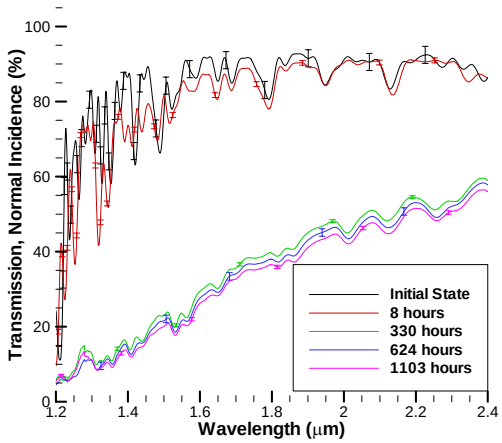

Filter ID: KX44-2b

Figure 10: Sb_2Se_3 Based Tandem Filters Tested at a Temperature of 212F (100C)

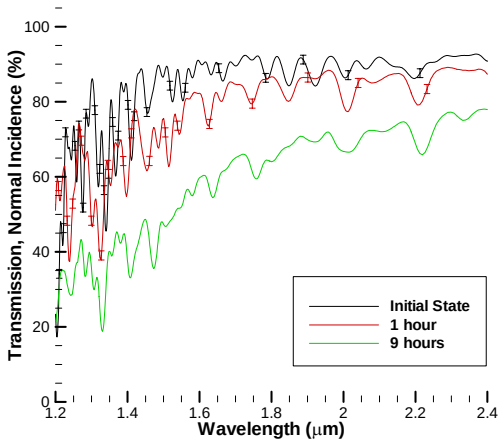

Filter ID: KX36-2

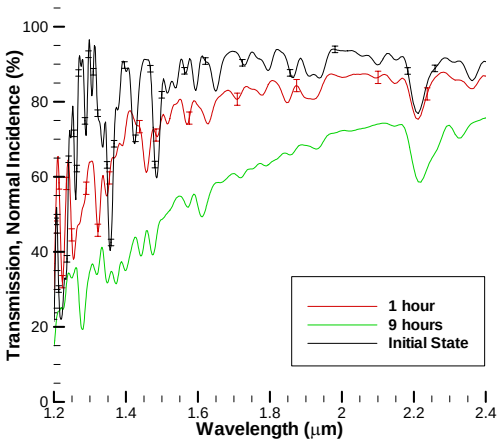

Filter ID: KX42-1

Figure 11: Sb_2Se_3 Based Tandem Filters Tested at Temperature of 230F (110C)

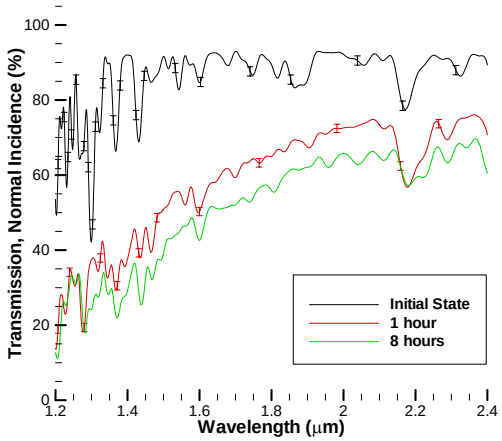

Filter ID: KX42-3a

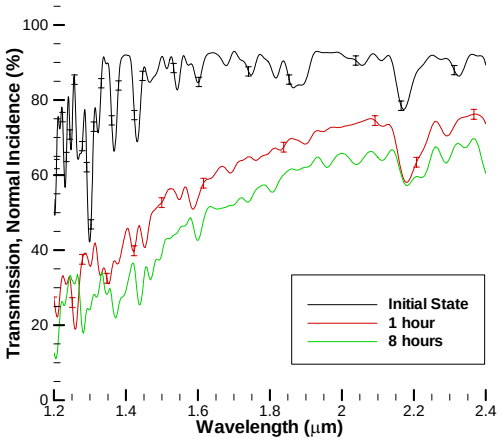

Filter ID: KX42-3b

Figure 12: Sb_2Se_3 Based Tandem Filters Tested at a Temperature of 248F (120C)

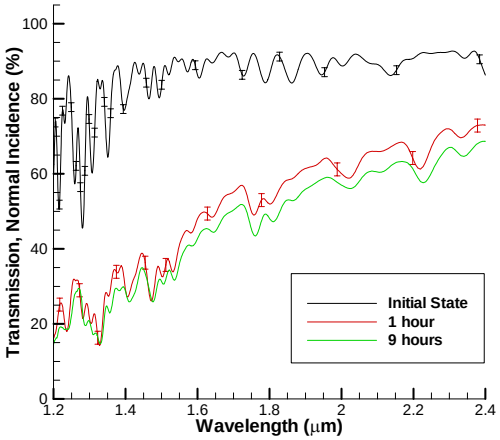

Filter ID: KX36-2

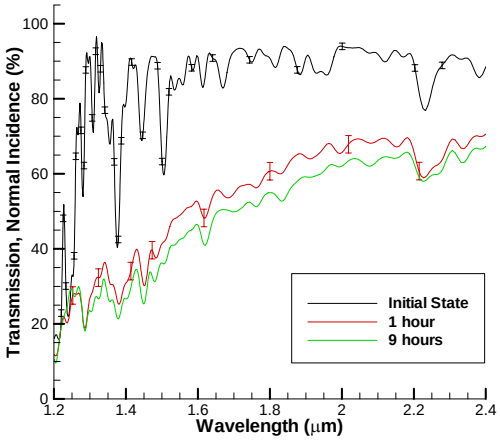

Filter ID: KX42-1

Figure 13: Sb_2Se_3 Based Tandem Filters Tested at a Temperature of 266F (130C)

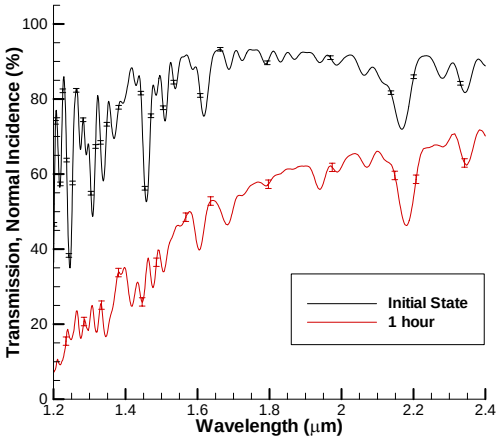

Filter ID: KX34-1

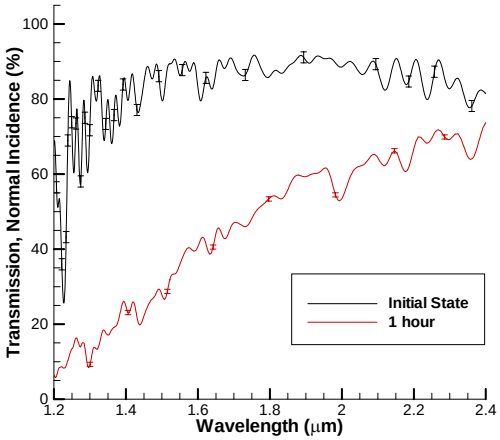

Filter ID: KX40-4

Figure 14: Sb_2Se_3 Based Tandem Filters Tested at a Temperature of 284F (140C)

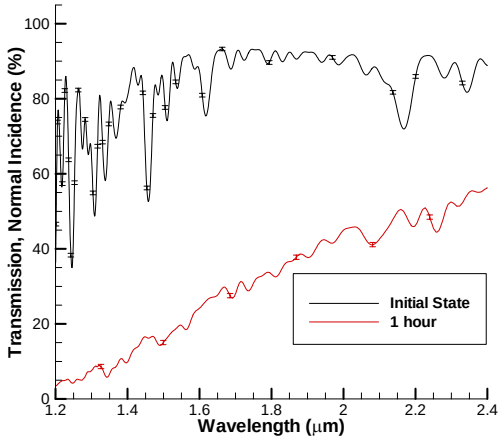

Filter ID: KX34-1

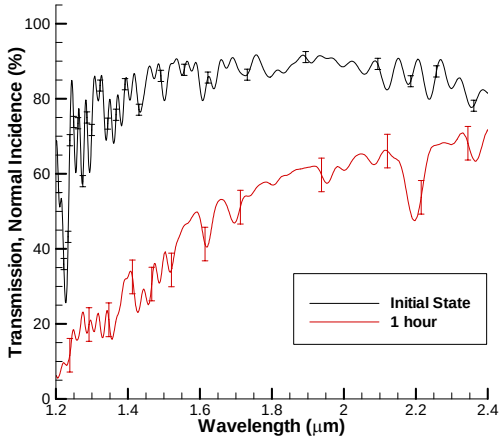

Filter ID: KX40-4

Figure 15: Sb_2Se_3 Based Tandem Filters Tested at a Temperature of 302F (150C)

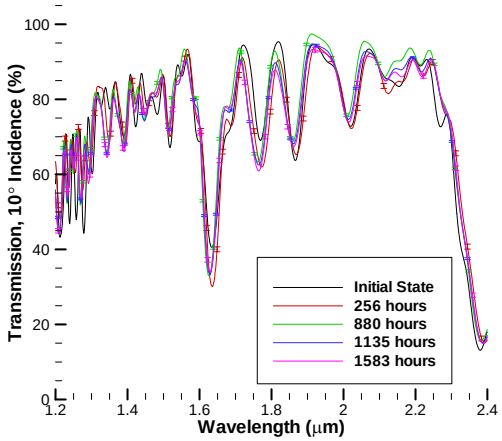

Filter ID: KE22c-1

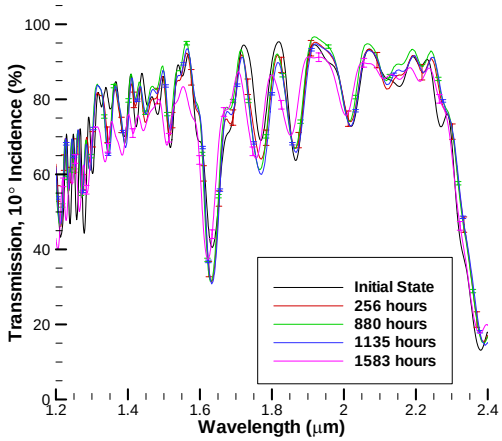

Filter ID: KE22c-2

Figure 16: GaTe Based Tandem Filters Tested at a Temperature of 302F (150C)

No change in the optical characteristics of the samples from the Sb_2Se_3 based tandem filters occurred at a temperature of 176F (80C) for 1150 hours and the GaTe based tandem filters at a temperature of 302F (150C) for 1583 hours. For these samples, the measurement uncertainty indicated by the error bars included all the measured data in general. At 212F (100C), however, the samples from the Sb_2Se_3 based tandem filters displayed an approximately 50% decrease in transmittance at a wavelength of 2μm after 330 hours. Subsequent baking of these samples from 330 hours to 1103 hours showed a smaller decrease in transmittance at a wavelength of 2μm. At 230F (110C), the samples from the Sb_2Se_3 based tandem filters displayed a rapid,

10% decrease in transmittance at a wavelength 2µm after 9 hours. The decrease after 1 hour at this temperature was less with some spectral regions showing no change as indicated by the measurement uncertainty that includes the initial state values. At 248F (120C) and 266F (130C), the samples from the Sb_2Se_3 based tandem filters displayed a rapid, 25% decrease in transmittance at a wavelength 2µm after 8 hours with most of the decrease occurring after only 1 hour. Finally, at 284F (140C) and 302F (150C), the samples from the Sb_2Se_3 based tandem filters displayed a rapid, greater than 25% decrease in transmittance at a wavelength 2µm after only 1 hour.

Given these results, Sb_2Se_3 based tandem filters can be operated at 176F (80C) or lower for at least 1000 hours before any changes in the optical characteristics of the tandem filter occur. In contrast, GaTe based tandem filters can be operated at 302F (150C) or lower for at least 1000 hours before any changes in the optical characteristics of the tandem filter occur. The GaTe based tandem filter may be able to be operated at even high temperature given the estimated instantaneous transformation temperature given in the previous section for GaTe and the other materials used in the optical interference coatings for the tandem filters. The Sb_2Se_3 based tandem filters can not operate at higher temperatures for 1000 hours given the results for the samples from Sb_2Se_3 based tandem filters at 212F (100C).

For the Sb_2Se_3 based tandem filters, any temperature excursions above 176F (80C) for as little as 1 to 10 hours will likely result in permanent decrease in the spectral transmittance and as a result the power output of a TPV energy conversion system. The magnitude of this decrease will depend on the temperature and the time at the temperature of the excursion.

Fabrication Trial of Co-Deposition of Sb_2Se_3 and Sb_2S_3

As an alternative approach to addressing the temperature stability of Sb_2Se_3, several co-deposition runs of Sb_2Se_3 and Sb_2S_3 were attempted based on the suggestion from a couple of external, independent experts. The postulation was that a combination of the two materials would yield a material with characteristics of the constituent materials, specifically the optical properties of Sb_2Se_3 and the higher temperature stability of Sb_2S_3. With co-deposition, two or more source materials (in this case Sb_2Se_3 and Sb_2S_3) are simultaneously evaporated in the physical vapor deposition process to achieve a new material (in this case a ternary $Sb_xSe_yS_z$). Three runs were completed by Rugate Technologies, Inc., and a ternary material was achieved based on scanning electron microscopy results as shown in Figure 17 and Figure 18. The next steps for developing this approach would be to determine the optical characteristics of the material and optimize the physical vapor deposition process for the desired optical characteristics.

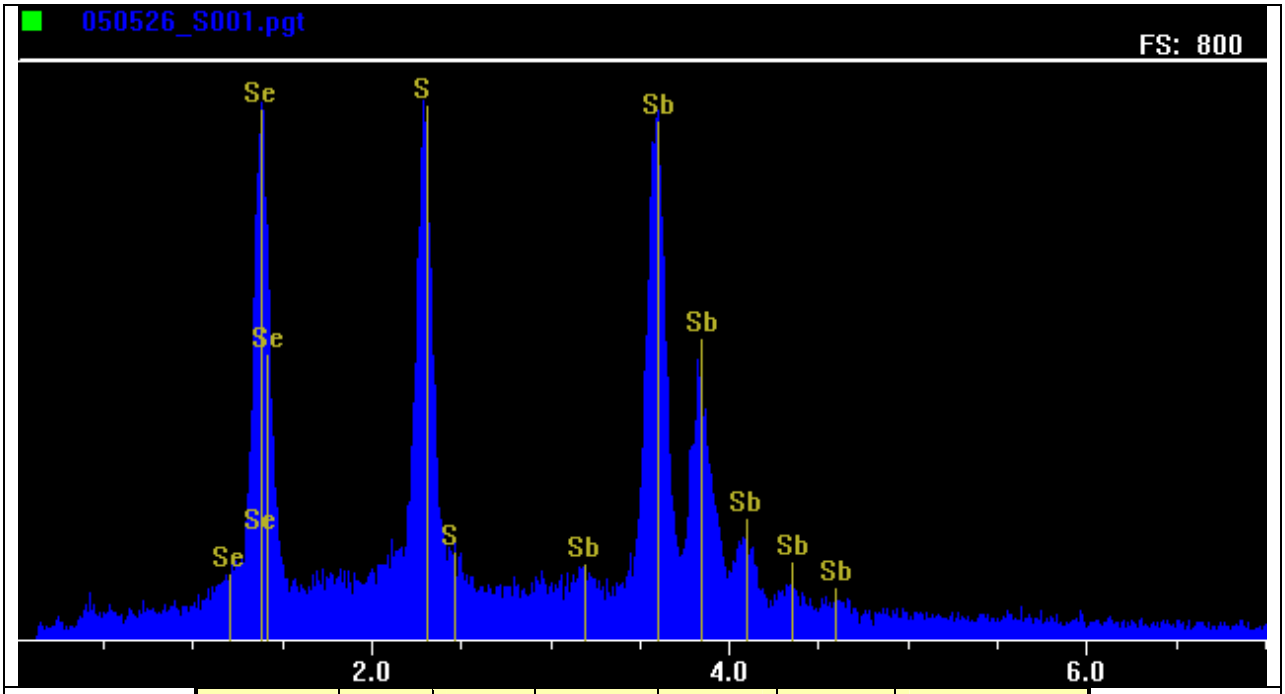

Element	Line	keV	KRatio	Wt%	At%	ChiSquared
Sb	LA1	3.604	0.5441	60.36	42.19	7.13
Se	LA1	1.379	0.2209	30.07	32.41	1.31
S	KA1	2.307	0.1035	9.57	25.40	1.64
Total				**100.00**	**100.00**	**3.73**

Element	Line	Det Eff	Z Corr	A Corr	F Corr	Tot Corr	Modes
Sb	LA1	0.935	1.082	1.025	1.000	1.109	Elmnt.
Se	LA1	0.877	0.990	1.377	0.998	1.361	Elmnt.
S	KA1	0.897	0.757	1.234	0.990	0.925	Elmnt.

Element	Line	Gross (cps)	BKG (cps)	Overlap (cps)	Net (cps)	P:B Ratio
Sb	LA1	243.2	36.8	0.0	206.5	5.6
Se	LA1	210.6	25.6	0.0	185.0	7.2
S	KA1	231.1	34.8	0.0	196.3	5.6

Live Time:	60.00	Count Rate:	2211	Dead Time:	22.68 %
Beam Voltage:	10.20	Beam Current:	0.30	Takeoff Angle:	26.93

Figure 17: Compositional Results for Co-deposition Sb_2Se_3 and Sb_2S_3

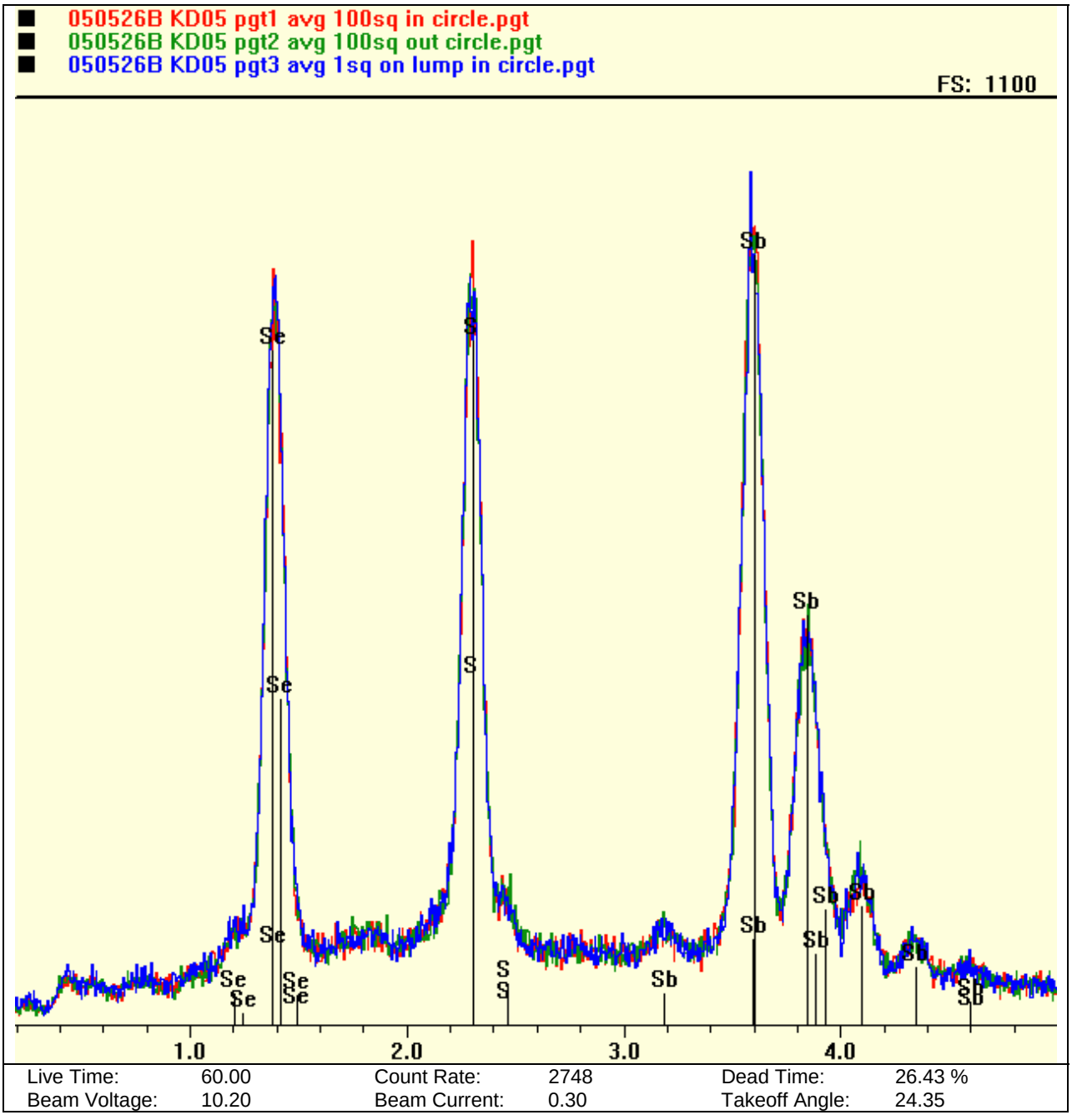

Figure 18: Spectral Results for Co-deposition Sb_2Se_3 and Sb_2S_3

Fabrication of Plasma Filters

The plasma filters are for now an essential component of a TPV tandem filter. The design of the plasma layer has been optimized and is defined by the technical specification used to procure the plasma filter that consists of an InP wafer with a single, epitaxially grown InPAs layer. Table 17 contains a summary of the plasma filter fabrication runs since 2003.

Table 17: Plasma Filter Fabrication Runs*

Date	Quantity	Wafer Diameter (inch)	Carrier Concentration Target (x 10^{19} cm^{-3})	Wafers per Run	Series IDs
2003 November	55	2	4.0-6.0	1	M5-67##
2004 March	15	2	4.0-6.0	1	M5-7153 – M5-7170
	5	2	2.0-3.0	1	M5-7172 –M5-7176
	5	2	3.0-4.5	1	M5-7177 –M5-7182
2004 September	55	2	4.0-6.0	1	M5-73##
2005 March	49	3	4.0-6.0	7	M1-1539(A-H) - M1-1545(A-H)
2005 March**	24	3	4.0-6.0	6	M1-1546(A-H) - M1-1549(A-H)

* Bettis also arranged for six (6) plasma filters on 2 inch diameter substrates to be fabricated by EMCORE. The fabrication specification and electrical performance was unknown, but these filters are numbered as '4cy-####'.

** Bettis procured these plasma filters using the same fabrication specification as KAPL's and the fabrication runs followed directly after the KAPL runs based on the series IDs.

The significance of fabrication variation, however, has been questioned. The design of the optical interference coatings is coupled to the performance of the plasma layer. Therefore, variation in the plasma filter fabrication could reduce the performance of the completed tandem filter. However, this variation, if significant, can be accommodated by refining the design of the optical interference coatings prior to depositing optical interference coatings on the plasma filter to create the tandem filter.

Compounding the difficulty in accessing the variation in the plasma filters is that plasma filters are fabricated based on electrical specifications; yet the performance of the plasma filters is based optical on characterization. Moreover, differences exist between the various optical techniques used to characterize the performance.

Resolving these issues is incomplete. Since the impact of the fabrication variation in the plasma filters is smaller than other considerations, resolving the issue has been a lower priority.

Fabrication of Multiple, Three Inch Diameter Plasma Filters

For the first time, plasma filters were fabricated on three inch diameter wafers, and during the same fabrication runs multiple wafers per run were successfully completed. Specifically, eleven[4] runs of seven or six plasma filters each were completed. Until then, the plasma filters were fabricated on two inch diameter wafers with one wafer per run. The larger wafers are required to minimize edge gap area that leads to parasitic photon absorption in large TPV arrays. The ratio of edge gap area to the overall array area decreases as the size of the wafer piece increases. In addition, with the plan to create larger TPV arrays, greater numbers of plasma filters would have been required. Moreover, fabricating multiple filters per fabrication run reduced the cost of the filters.

Fabrication of Plasma Filters with Lower Doping Levels

Rugate Technologies, Inc. suggested that lower doping (carrier concentrations) in the InPAs layer (plasma filter) may allow higher tandem filter performance. The carrier concentration influences the plasma wavelength shown in Figure 19. If the carrier concentration was reduced and the plasma wavelength shifted to longer wavelengths, the resulting gap in the required, high reflection of below band gap photons could be accommodated by the design of the optical interference coatings. If so, then the lower carrier concentration would decrease the optical absorption in the plasma filter and thus improve the performance of the tandem filter.

[4] As shown in Table 17, seven of the eleven runs were contracted to Bandwidth by KAPL, and the remaining four runs were contracted to Bandwidth by Bettis. The same technical specification was used, and the runs occurred consecutively using the same fabrication system. The only difference was the InP wafers used. The KAPL runs used Nikko wafers provided by Bandwidth, and the Bettis runs used Sumitomo wafers provide by Bettis.

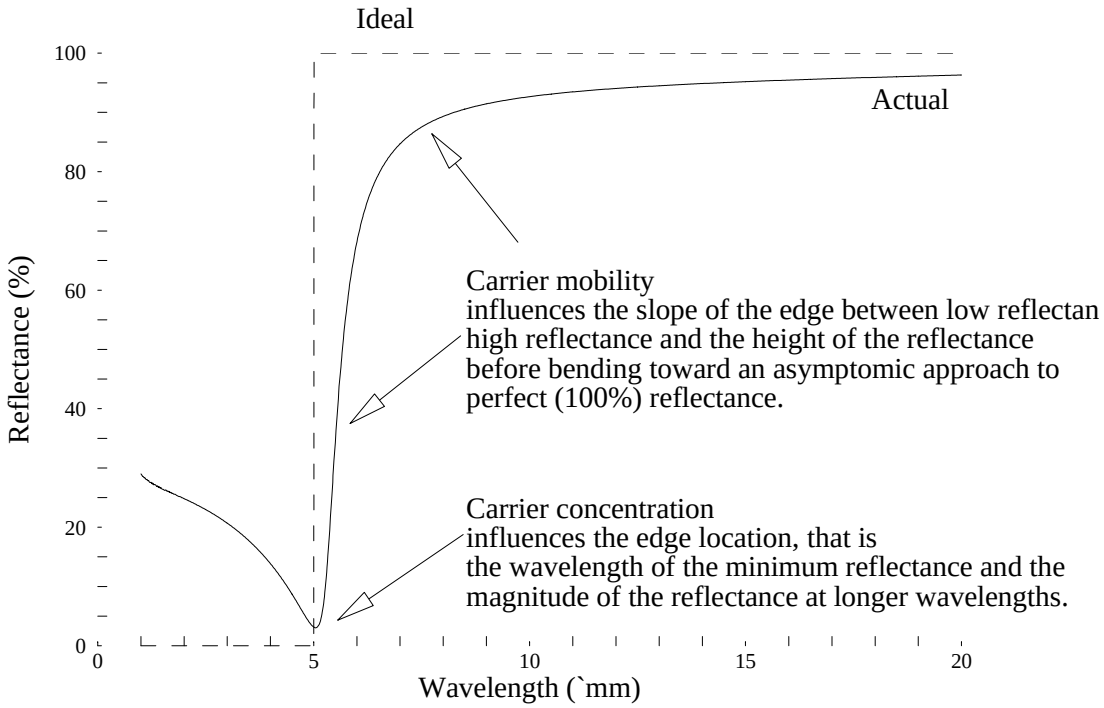

Figure 19: Optical Performance of $InP_xAs_{(1-x)}$ Layer on an InP Substrate

As shown in Table 17, several plasma filters were fabricated with 50% and 75% of the normal carrier concentration in order to test this idea. Representative tandem filters were then characterized optically using spectroscopic ellipsometry as with all plasma filters. Using the measured optical performance of these plasma filers, the tandem filter performance was optimized using the filter defined edge configuration. To summarize, the performance of the tandem filter with the lower carrier concentrations in plasma filter were lower than with plasma filters with the normal carrier concentrations. This analytical result has yet to be confirmed experimentally by fabricating tandem filters using the plasma filters with the lower carrier concentration. Furthermore, the analytical result is limited to the '767' design architecture assumed in the analysis and is constrained by the number of layers used in the analysis. A design analysis with a different architecture and more complexity (more layers) may show an improved performance is possible.

Optical Characterization of Tandem Filters

Questions arose about the reflectance characterization of the tandem filters when spectral reflectance values greater than 100% (that is, non-physical) began to be consistently measured. The concern was primarily with the spectral reflectance characterization rather than the spectral transmittance characterization. However, along the way, problems associated with both reflectance and transmittance measurements were identified. Concern with the optical characterization of the tandem filters is not a new problem. As the performance of the fabricated, tandem filters increased, the concern with accuracy and precision of the measured reflectance and transmittance increased. In order to provide useful feedback to the tandem filter

development process, excellent precision and accuracy (<1% uncertainty) of the measured, spectral reflectance and transmittance of the tandem filters are desired.

Therefore, considerable effort was spent to ensure the veracity of the measured performance of the tandem filters. An attempt was made to question every aspect of the characterization process. The conclusions and the observations that resulted follow:

- The precision (repeatability of the given measurement) of the reflectance characterization using the FT-IR spectrometer is sufficient, but the reflectance characterization using the dispersive spectrometer in its current configuration is problematic. On the other hand, the precision of the transmittance characterization using the FT-IR spectrometer is problematic, especially at incident angles near normal (0°). The precision of the transmittance characterization using the dispersive spectrometer in its current configuration is sufficient only at normal (0°) incident angles but is problematic at all other incident angles.

- The accuracy (closeness of the given measurement to the true, but unknown, value) of the reflectance characterization using the FT-IR spectrometer is uncertain, and the reflectance characterization using the dispersive spectrometer in its current configuration is problematic. Furthermore, the accuracy of the transmittance characterization using the FT-IR spectrometer is also uncertain, especially at incident angles near normal (0°). The accuracy of the transmittance characterization using the dispersive spectrometer in its current configuration is sufficient only at normal (0°) incident angles but is problematic at all other incident angles.

Table 18 summarizes these conclusions. In this table, the performance of the spectrometers is qualitatively judged to be sufficient, problematic, or unknown. Spectral characterization is sufficient if the precision or accuracy is judged to be appropriate for the current stage of spectral control development and insufficient if the precision or accuracy is judged to be inappropriate for the current stage of spectral control development. The accuracy of the spectral reflectance measurements using the FT-IR spectrometer is judged to be unknown as several issues need to be addressed to prior to quantifying the accuracy. These issues include reflectance standards, random polarization, instrument errors, and operational procedures.

Table 18: Qualitative Performance of the Spectrometers Used to Characterize the Optical Performance of the Tandem Filters

Spectral Characterization	Spectrometer	**Precision**	**Accuracy**
Reflectance	FT-IR	Sufficient	**Unknown**
	Dispersive	Insufficient	Insufficient
Transmittance	FT-IR	Insufficient, 0-9° AOI, Sufficient, 10-80° AOI	Insufficient, 0-9° AOI, **Unknown**, 10-80° AOI
	Dispersive	Sufficient, 0° AOI, Insufficient, >0° AOI	Sufficient, 0° AOI, Insufficient, >0° AOI

The following subsections provide a more detailed discussion of the identified issues associated with the optical characterization of the tandem filters. In the end, the ultimate characterization of the tandem filter performance is a TPV module test that directly measures the energy conversion performance of a tandem filter together with a TPV cell. The results from 0.25-0.5W TPV module tests suggest that the accuracy of the spectral reflectance characterization of the tandem filters using the current configuration of the FT-IR spectrometer is sufficient to be used for predictions/models of these TPV modules. In addition, the accuracy of the spectral reflectance characterization is expected to be sufficient for larger arrays of TPV modules as well.

<u>Implementation of Periodic Evaluations of the Au Working Standard for Reflectance Measurements Using the FT-IR Spectrophotometer</u>

After some effort and false starts, degradation of the working Au standard used for the spectral reflectance measurement with the Fourier Transform infrared (FT-IR) spectrometer was identified as the primary reason for the non-physical, greater than 100% spectral reflectance measurements. For spectral reflection, the FT-IR spectrometer provides a relative measure of reflection rather than an absolute measure of reflection. In other words, the FT-IR spectrometer measures the relative intensity of reflected light from a working standard, supposedly of known reflection, with the intensity of reflected light from the sample surface. The corrective actions identified and implemented to minimize the error due to degradation of the working standard are as follows:

1) The working standard must be periodically compared to the pristine standard to check if degradation has occurred. Degradation would mean the working standard has relative reflectance compared to the pristine standard of less than 1.0 across the spectral range of interest. If so, the working standard must be replaced with a new working standard that does match the reflectance of the pristine standard.

2) The working standard and the pristine standard must be the same size, shape, and weight. The pristine standard is the Au surface that has been independently measured

relative to a National Physical Laboratory[5] (NPL) standard and is to be used only for characterization and qualification of the working standard. Initially, the degraded working standard was compared to pristine standards of different size and weight. Inconsistent measurements resulted. Later it was determined that the way the standard rests on the horizontal sample stage can significantly alter the measured reflectance. A thickness of cellophane tape placed such that one side of the sample is raised as compared to the other side results in a measurable difference in reflectance. Hence, the working standards and the pristine standards must be the same size, shape, and weight.

In general, these corrective actions eliminated the non-physical, greater than 100% spectral reflectance measurements and therefore improved the accuracy of the measured, spectral reflectance. The precision of the measured, spectral reflectance was likely improved, also, but the precision was sufficient with the degraded working standard as the results of a repeated measurement of a tandem filter suggests. Figure 20 shows the results of a repeated measurement of a tandem filter that had been measured originally two years earlier using another degraded, working standard. The differences in the figures of merit from each measurement are less than one percent, suggesting that the precision, but not necessarily the accuracy, with degraded working standards was sufficient.

[5] The National Physical Laboratory is the United Kingdom's equivalent to the U.S.' National Institute of Standards and Technology (NIST).

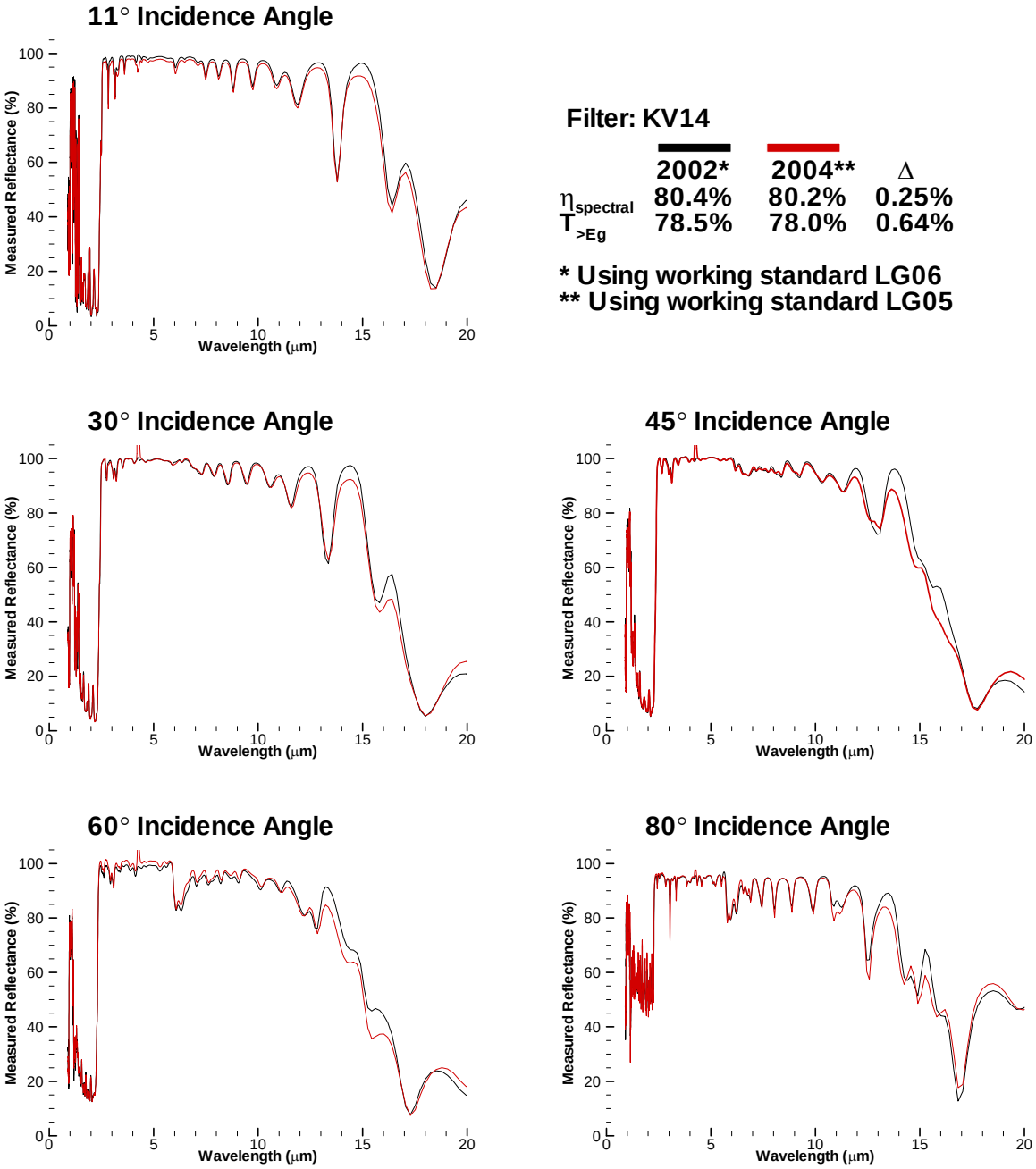

Figure 20: Re-Measured Tandem Filter

Assessing the Spectral and Directional Reflectance of the Au Standard

The spectral and directional reflectance of the Au standard (working or pristine) used to calculate the relative reflectance of a sample has been questioned. To date, a constant value, 0.985, for the spectral reflectance for all incident angles of the pristine standard has been used. However, the reflectance of Au is spectrally and directionally dependent.

The optical response of a material is caused by the interaction of the electromagnetic wave and the charge carriers in the material. From the optical properties listed in Palik (Reference (7)), Figure 21 shows the spectral and directional variation of the reflectance of Au.

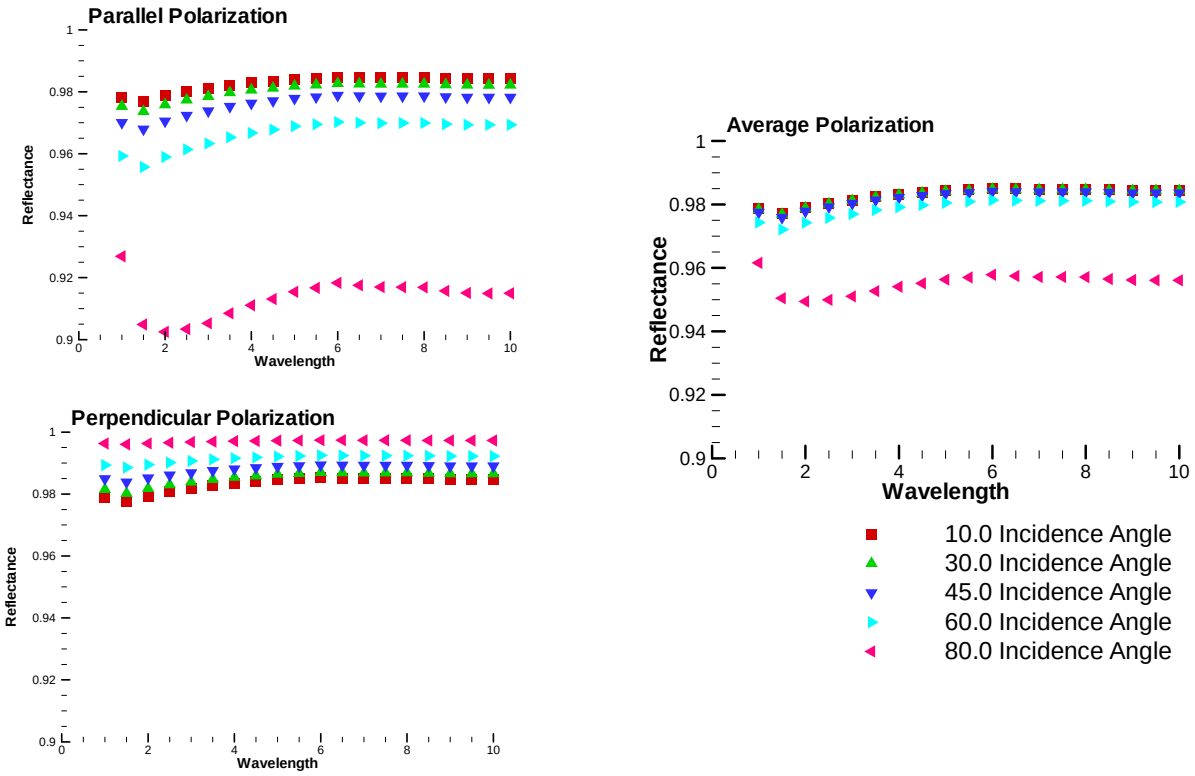

Figure 21: Spectral and Directional Variation of Au (Reference (7))

Furthermore, the Hemispherical Directional Reflectometer (HDR) system from Surface Optics uses the spectral and directional variation shown in Figure 22 for the Au standard within the HDR system to determine the reflectance based on the measured relative reflectance.

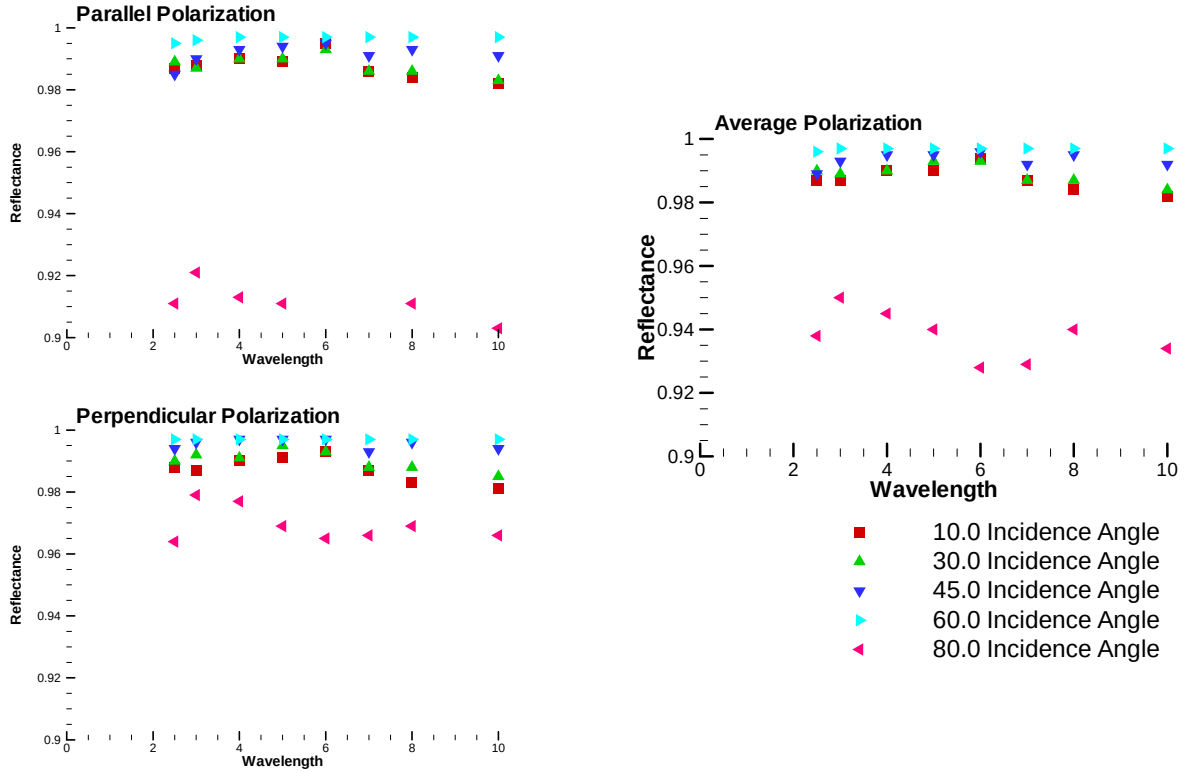

Figure 22: Spectral and Directional Variation of Au for Hemispherical, Directional Reflectometer (HDR)

Optical Data Associates (ODA), LLC was contracted to measure the spectral reflectance of a representative sample from two batches of Au mirrors fabricated for KAPL, one batch in 1999 and another batch in 2004. These Au mirrors are used as the pristine and working Au standards for the relative spectral reflectance measurements using the FT-IR spectrometer. ODA uses a reflectance reference standard from UK's National Physical Laboratory (NPL) to characterize the absolute reflectance of KAPL's Au mirrors at a near normal incident angle. The results are compared in Figure 23. The spectral reflections shown in the figure represent the average of two measurements for each Au mirror. Two different spectrometric systems were used to measure the spectral reflectance: one system was used to measure from the ultraviolet (UV) to the visible (VIS) spectra, and another system was used to measure from the near infrared (NIR) to the infrared (IR) wavelength spectra.

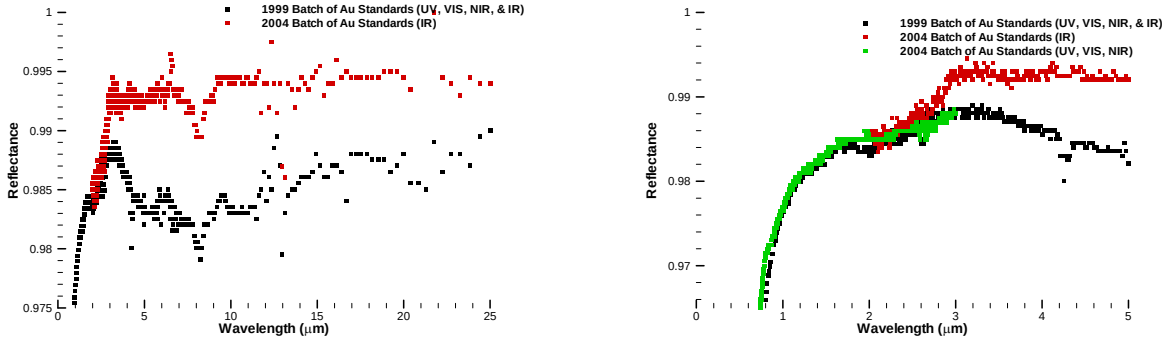

Figure 23: Comparison of the Spectral Reflectance (Near Normal Incidence) of KAPL Au Standards

The measured reflectance shows a spectral dependency. In addition for the infrared region, the measured reflectance of the 2004 sample is slightly higher than the measured reflectance of the 1999 sample. Although KAPL is skeptical, the principal investigator at ODA judged the difference to be significant relative to the uncertainty of the measurements. The measured reflectance in the ultraviolet, visible, and the near infrared regions are similar and show no significant differences.

A spectrally and directionally dependent reflectance for both polarizations of the Au standards may increase the accuracy of the relative spectral and direction reflectance measurements using the FT-IR spectrometer. The impact of neglecting these differences has yet to be determined. Except for the spectral reflectance at 80 incident angle, the difference in the spectral reflectance values would be at most 1% (99.5% instead of 98.5%) at limited wavelength regions. On the other hand, an absolute measurement of spectral and directional reflectance would eliminate the need for reflectance standard, like the Au mirrors. The potential of absolute spectral and directional reflectance measurements is discussed later.

Assessing the Limitations of Optical Characterization with Random Polarization

The degree of randomization of the polarization of the signal from a spectrometer may vary with time and vary between instruments. A representative of a manufacturer of FT-IR accessories (Harrick) suggested the need to measure each component of electromagnetic radiation separately. The Surface Optics Hemispherical, Directional Reflectometer (HDR) system procedure measures and reports each component separately. Finally, an expert (Hanssen, NIST) on spectral reflectance characterization in the infrared measures and reports each component separately.

In contrast to the practice used currently to characterize the performance of the tandem filters, a procedure to measure and report each component of electromagnetic radiation separately should be considered. The average of the components of electromagnetic radiation could then be calculated, if desired. Figure 24 shows the difference for the spectral reflectance of an InP wafer measured in the FT-IR with a polarizer to measure each component separately and the measurement using the ‘as is’ randomized polarization of the FT-IR.

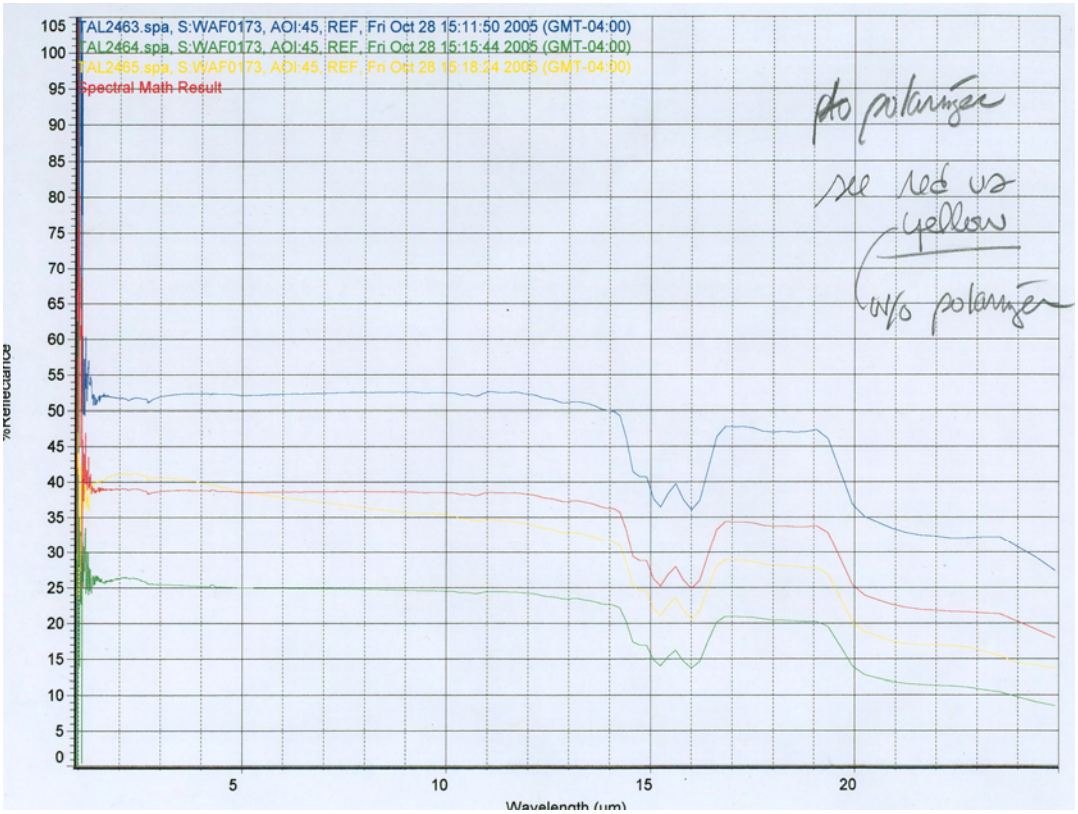

Figure 24: Comparison of Measured Spectral Reflection with 'As Is' Random Polarization (—) and the Average of Separately Measured Components of Electromagnetic Radiation Using a Polarizer (—)

The difference is 5% at 2µm, zero at 5µm, and 11% at 10µm. The impact of this potential difference on the accuracy of the measured, spectral reflectance is estimated to be ±1-2% of spectral efficiency based on previous estimate of measurement uncertainty. Finally, both the dispersive spectrometer and the FT-IR spectrometer suffer from this degree of randomization uncertainty.

Assessing the Limitations of the Fourier Transform Infrared (FT-IR) Spectrometer

The Fourier Transform infrared (FT-IR) spectrometer has been and still is the characterization tool used to measure spectral reflectance and transmittance of tandem filters. Shortcomings exist for using the FT-IR spectrometer for spectral reflectance and transmittance characterization. Measurement uncertainty of the accuracy of the reflectance and transmittance measurements using the FT-IR spectrometer has been estimated to be ±1.5% and determined to be significant relative to spectral efficiency. However, this estimate of uncertainty is questionable given the issues about the accuracy of the measured, spectral reflectance or transmittance using the FT-IR spectrometer that have been identified as part of this extensive testing and evaluation of the instrument. To be clear, only the accuracy of the magnitude of the measured, spectral reflectance and transmittance using the FT-IR spectrometer has been questioned. The precision of the magnitude of the measured, spectral reflectance and

transmittance (for incident angles greater 10°) using the FT-IR spectrometer have been judged to be sufficient. Furthermore, the precision and accuracy of the measured, spectral location of the peaks and valleys of the reflectance and the transmittance are generally judged to be high with all FT-IR spectrometers.

The fundamental limitation of the FT-IR spectrometer is the linearity of the detector window and the associated focusing mirror for the detector. The linearity refers to the consistency of the measured intensity of photons striking different locations on the detector window and the associated focusing mirror. Ideally, the measured intensity of a photon flux striking any location on the detector and the associated focusing mirror should be equal. An error occurs when the indicated intensity of a given photon flux striking different locations on the detector or the associated focusing mirror varies. This error is often referred to as an alignment error (Reference (8)). For the tandem filters, the lack of surface flatness, the lack of parallelism between the two exterior surfaces, and the back surface reflectance can lead to slight shifts in the photon beam and hence the location where it strikes the detector and the associated focusing mirror. In addition, alignment of the filter in the reflectance and transmittance fixtures used with the FT-IR spectrometer can also lead to slight shifts in the photon beam and hence the location where it strikes the detector and the associated focusing mirror.

For example, the photon beam from the reflectance standard may not strike the same location on the focusing mirror for the detector as the photon beam from the sample due to the light path through the reflectance fixture or different tilt of the sample relative to the reference. No error would occur if the focusing mirror and detector indicate the same intensity regardless of where the photon flux strikes the focusing mirror and the detector window. Otherwise, an error develops in the reflectance and transmittance measurement. A test using a fixed incidence angle fixture and variable angle fixture for the same incident angle in the FT-IR spectrometer to measure the spectral reflectance of an InP wafer showed a difference. Figure 25 shows an example of this difference between the measured reflectance of an InP wafer using a fixed angle accessory and a variable angle accessory on the FT-IR spectrophotometer.

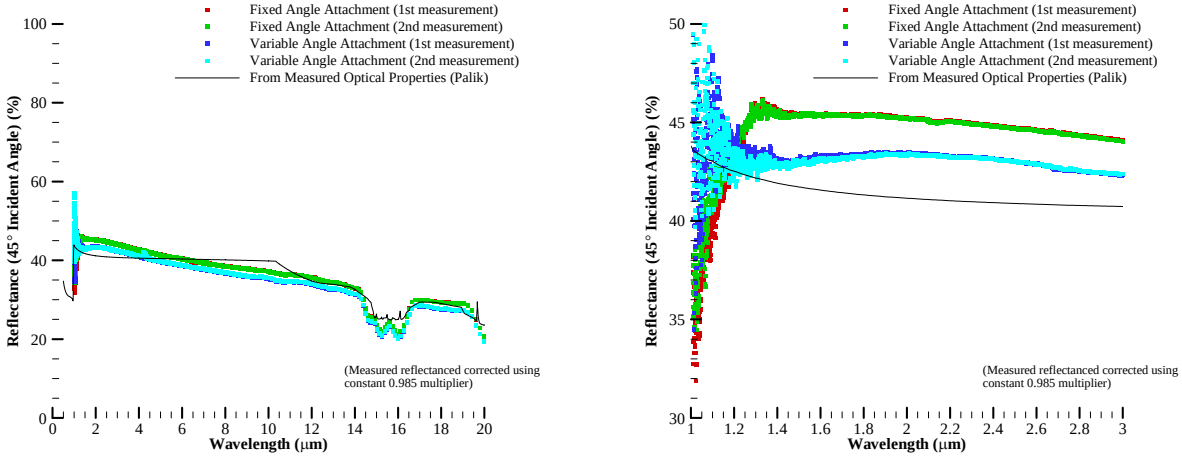

(Full Scale) (Detail)

Figure 25: Comparison of the a Fixed Angle and Variable Angle (Seagull) Accessories for Spectral Reflection Using the FT-IR Spectrometer

At 2μm, the difference is about 4% and is roughly consistent through most of the displayed wavelength range. The reason for the difference is suspected to be the alignment error just described.

Moreover, a comparison between spectral and directional reflectance measured by KAPL and Rugate Technologies, Inc. using the same tandem filters, identical working standards, similar FT-IR spectrophotometers, and identical variable angle reflectance accessories (Harrick Seagull) was completed. Rugate Technologies, Inc. had three different individuals measure each filter. The results are shown in Figure 26. Two sets of results for each measurement are provided. The 'baseline' or 'as-measured' results represent the performance with only the Au reflectance correction (0.985) applied to the measure spectral reflection data. In addition to this correction, the 'adjusted' results represent the performance with a shift of the spectral reflection data so that the peaks reach about 99.99%.

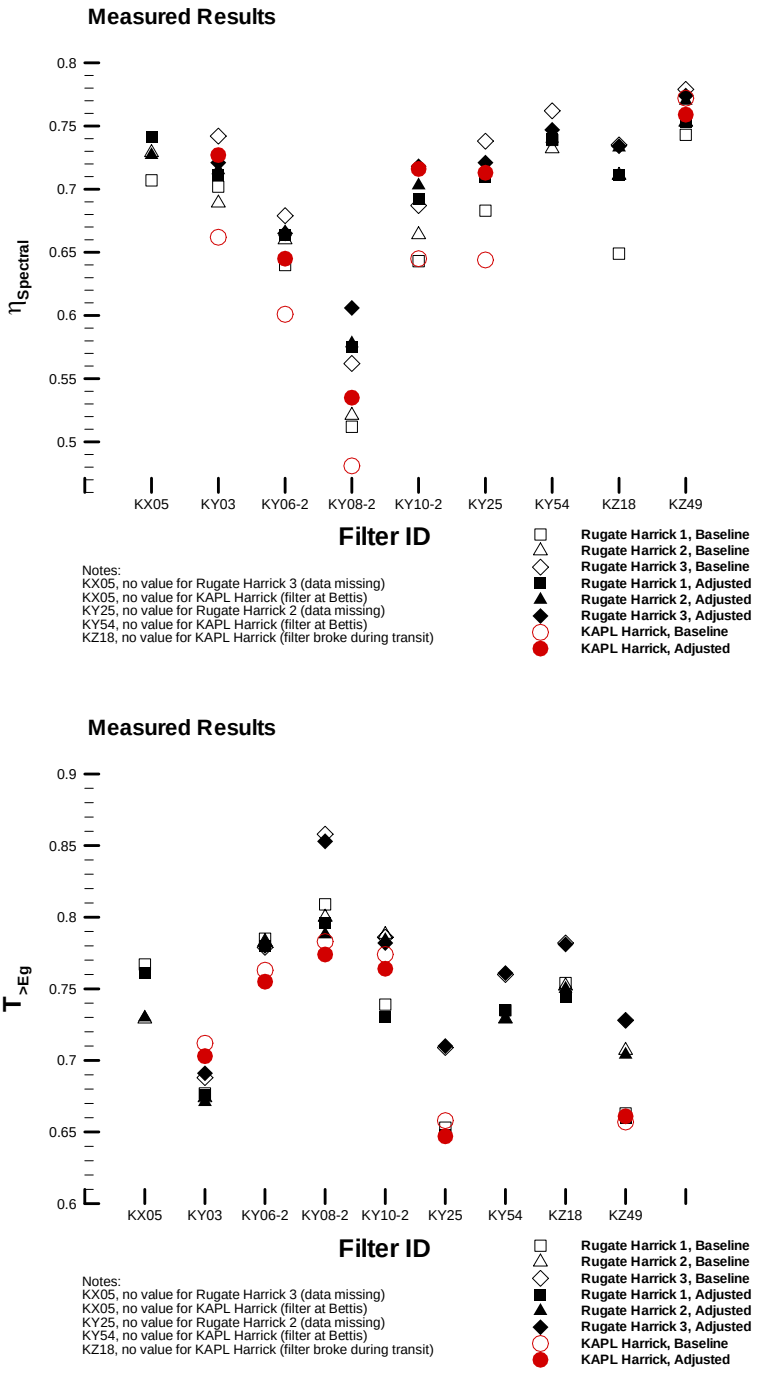

Figure 26: Comparison of Measured Reflectance Between KAPL and Rugate Technologies, Inc.

Differences as large as 10% resulted from the comparison. As discussed in the previous section, the use a polarizer to measure each component of the electromagnetic energy separately may improve the results and reduce the measurement differences. The magnitude of the improvement, if any, is uncertain.

The basis for including the 'adjusted' measured results in this section as well as throughout this report is the uncertainty of the accuracy of the directional, spectral reflectance measurement using the FT-IR spectrophotometer. The 'baseline' or 'as-measured' results represent the performance with only the Au reflectance correction (0.985) applied to the measure spectral reflection data. The 'adjusted' results represent an additional shift of the as-measured spectral reflection data so that the peaks reach about 99.99% reflectance. Figure 27 shows a comparison of as-measured and adjusted measured results for a representative tandem filter.

The as-measured results are suspect, since the magnitude of the peaks varies inconsistently with the incident angle. From Figure 27, the magnitude of the as-measured peaks varies from ~94.5% reflectance at an incident angle of 11° to ~99.5% reflectance at an incident angle of 60°, and then back to ~93% reflectance at an incident angle of 80°. No physical interpretation of these variations in the magnitudes of the peak reflectance could be identified. If undesirable absorption appeared in one or more of the materials used for the optical interference coatings, then a general decrease in the magnitude of the reflectance peaks would be expected as the incident angle increased. Specifically, the peaks for the incident angle of 11° would be the highest and the peaks for the incident angle of 80° would be the lowest with a general decreasing trend for other incident angles between these two incident angles. This expectation is based on the path length for the photons traveling into and out of the tandem filters. For an incident angle of 11°, the path length is shorter than the path length at an incident angle of 80°. The absorption and the corresponding decrease in reflectance increases as the path length increases.

In the end, the adjusted measured results represent an upper bound of the measured performance. How close the real performance is to this upper bound is uncertain.

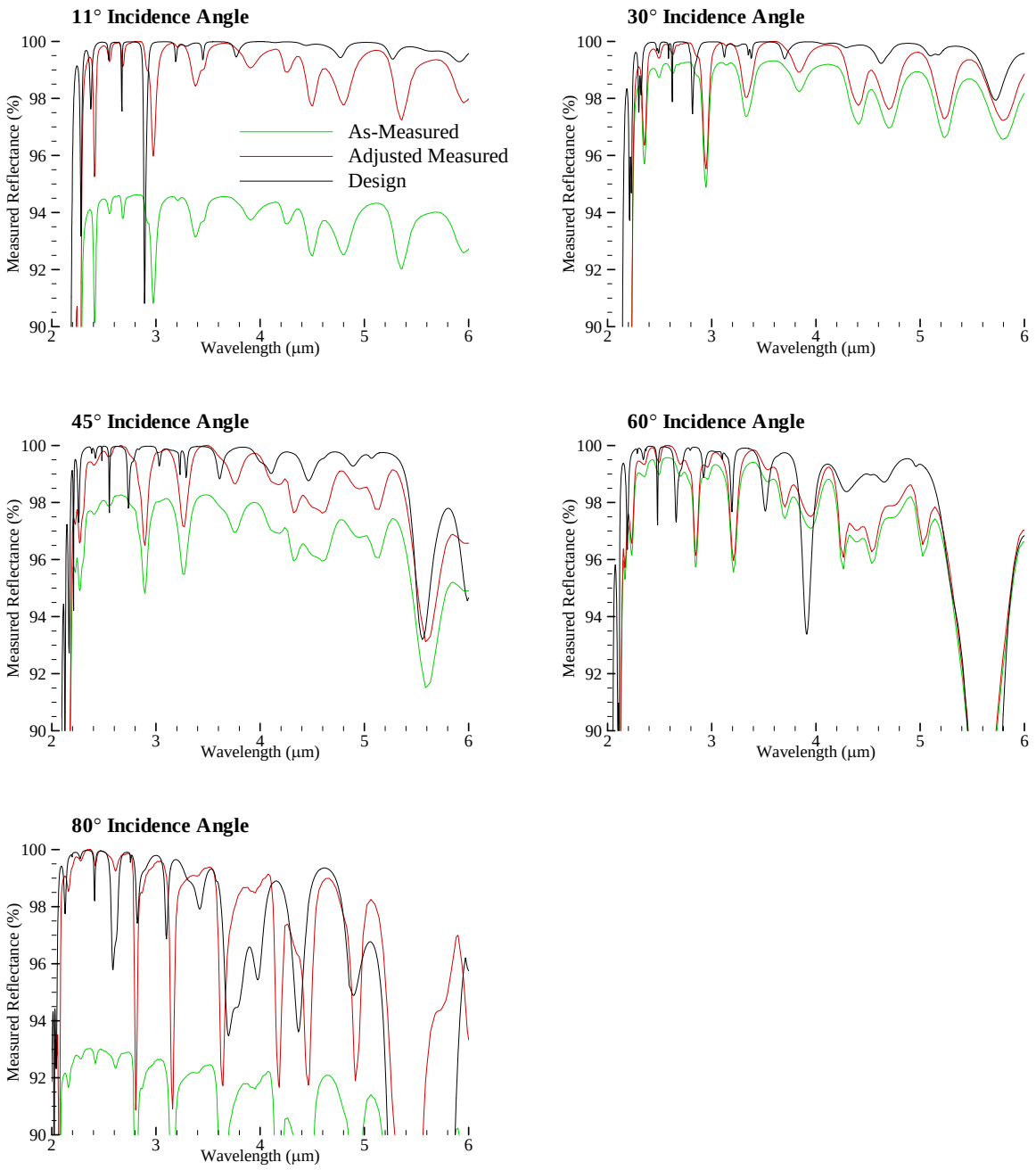

Figure 27: Comparison of the As-Measured and the Adjusted Results for a Representative Tandem Filter

Finally, another uncertainty associated with near normal transmittance measurements using the FT-IR spectrometer was identified. Specifically, transmittance measurements for incident angles of about 6° or less introduce a so called 'retro reflection' error (Reference (9)) where a fraction of the light reflects from the sample back into the instrument and then incorrectly augments the measured energy level after this light passes back through the sample to the detector. Fixtures are now offered to mitigate this error, but for now the dispersive spectrometer can be used for normal incidence, spectral transmittance measurements as mentioned later.

Lenord Hanssen at the National Institute of Standards and Technology has developed spectral reflectance and transmittance measurement systems that seem to mitigate the uncertainties associated with the current spectral reflectance and transmittance measurements using the FT-IR spectrometer. Interestingly, Dr. Hanssen's system uses an FT-IR as the source. Using a Si wafer of known properties as an absolute reflectance standard to assess the accuracy of a spectral reflectance measurement system, Dr. Hanssen has achieved an accuracy of 0.1-0.2% reflectance and transmittance for a spectral region from 2-5µm for incident angles from 12-80° (Reference (10)) using a goniometer configuration and 0.2-0.4% reflectance and transmittance for a spectral region from 1-18µm for incident angles from 2-75° using an integrating sphere configuration (Reference (11)). Either of these configurations may improve the spectral reflectance and transmittance characterization of the TPV tandem filters and could be assessed.

Assessing the Limitations of the Dispersive Spectrometer

The dispersive spectrometer as currently configured was determined to be working correctly but insufficient for measuring the spectral reflectance at various angles of incidence. The dispersive spectrometer was procured to provide absolute characterization of spectral and direction reflectance and transmittance. Depending on the size of the active area of the detector window, the dispersive spectrometer may introduce an error for spectral transmittance measurement at non-normal incidence angles due to the shift of the incident photons after passing through the specimen and the slight misalignment due to the required rotation of the specimen and the detector. A similar error could be introduced for spectral reflectance measurements as well. These conclusions are based on extensive testing and evaluation of the spectrometer following the guidance from a short course by the Optical Society of America, "Spectrophotometry – Instruments, Traceability, and Best Measurement Practices". Although costly (~$500-1000K), a likely solution would be a spectrometer that allows slight, multi-degrees-of-freedom alignment of the specimen to maximize the signal at every specimen and detector position. In other words, at any incident angle, the specimen could be automatically rotated about its axes to realign the reflected or transmitted incident photons to the center of the detector window and thus maximize the signal.

On the other hand, the dispersive spectrometer can be used and was used to measure spectral transmittance at normal incidence to compliment the use of the FT-IR spectrometer given the error associated with normal incidence transmittance measurements using the FT-IR instrument (described previously).

TPV Module Fabrication Using Tandem Filters

Several initiatives were implemented to support the fabrication of TPV modules using the tandem filters. The development of the two fabrication steps for the tandem filters required to assemble TPV modules is described next. In addition, later in this section, an assessment of TPV module failures potentially attributed to these fabrication steps is discussed.

Development of Trimming Techniques and an Adhesive Application System for the Fabrication of TPV Modules Using Tandem Filters

The current TPV module configuration requires two processing steps for the fabricated tandem filters. First, the tandem filters are trimmed into square or rectangular pieces to cover the TPV cells. Since many tandem filter pieces are required to be placed next to another, the quality of the edges is crucial to minimize discontinuities. Second, the tandem filter pieces are held in place on the TPV cells with an optical adhesive. Control of the adhesive thickness is essential to minimize absorption and allow the adhesive to fill gaps and discontinuities in the surface of the TPV cell arrays. Although these steps have been successfully performed in the past, development of the trimming and adhering process for tandem filters was completed to support the fabrication of the Small Array Test (SAT).

The optimum process for trimming the tandem filters (scribing and cleaving or dicing with a wafer saw) is uncertain and more development will be necessary to determine the optimum process. Both processes are used in the fabrication of semiconductors, so off-the-shelf production fabrication systems are readily available.

An optical adhesive application system was developed and implemented by Josef Parrington for the fabrication of the SAT. The system successfully controlled the thickness of the adhesive layer and allowed the use of profilometry data from the as-built array to vary the thickness of the adhesive under each tandem filter piece to achieve a level incident surface. The height of the fabricated TPV cell was slightly uneven and adjusting the adhesive thickness while applying the tandem filter compensated for the unevenness.

Identification of the Potential Cause of TPV Module Failures at the TPV Cell / Tandem Filter Interface

Four TPV module failures have occurred during the development of TPV energy conversion. A module failure refers to an abrupt change in the measure electrical and heat transfer properties while the module is illuminated. Although the cause of the failures is uncertain, delamination of the tandem filter from the TPV cell has been postulated as the cause or one of the causes of these failures. Therefore, the failures may be related to the fabrication steps involving the tandem filters. To begin to address the potential role of the tandem filters in these failures, the following complementary studies and a fabrication change were initiated:

- Analytical assessment of the thermal stresses within a TPV module,
- Experimental study of the allowable stress between adhesive interfaces,
- Implementation of alternative, anti-reflection coatings for the tandem filters.

First, to assess the interface stress level in a representative thermophotovoltaic module, a finite element analysis of the thermal stresses induced by the change in the isothermal temperature in the module at fabrication to the isothermal temperature in the module at the reference operating state (125F) was completed. The conclusion of the study was that the epoxy layer is causing the majority of the interface stress in the TPV module due to the large coefficient of thermal expansion difference between the epoxy material and the other materials in the module. Therefore, an alternate adhesive should be identified and implemented to reduce these stresses and perhaps mitigate TPV module failures.

Second, an experimental study to determine the allowable interfacial stress between the adhesive and the wafers was designed and implemented. Two identical sets of samples were created with representative interfaces between the tandem filters and the optical adhesive. Specifically, to represent the tandem filters, the existing (different than the anti-reflection coatings described in the next section) anti-reflection coatings were applied to multiple, one inch diameter InP wafers using two optical interference coatings runs. Two of the wafers from the same run were then joined with the actual adhesive and the actual adhesive application process. A sketch of the resulting samples is show in Figure 28.

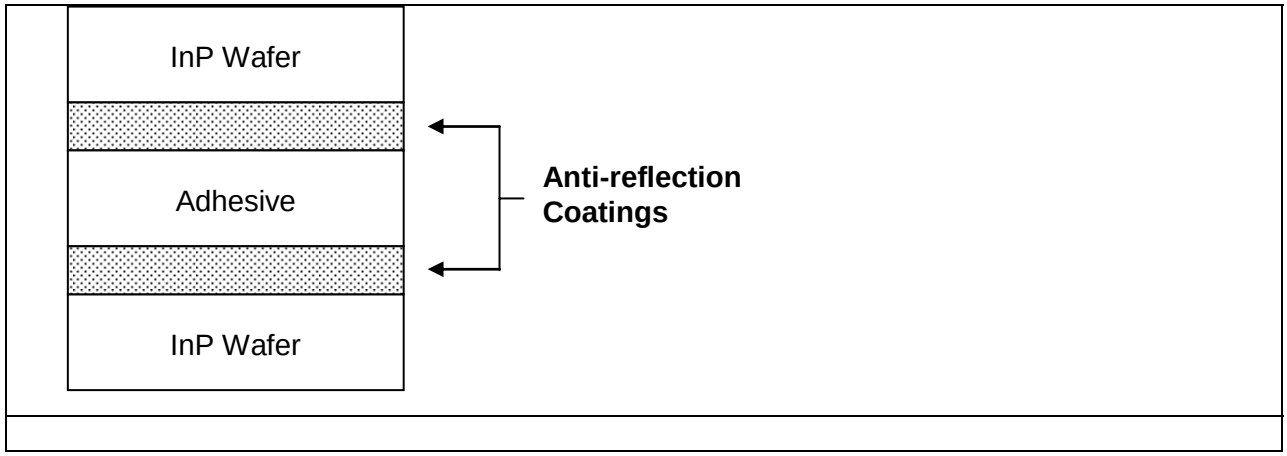

Figure 28: Configuration of the Symmetric Samples for Interface Strength Studies

Two samples, one from each set of samples, were uniformly heated from room temperature in a vacuum oven to various temperatures and held for two hours at temperature before cooling back to room temperature as summarized in Table 19.

Table 19: Adhesive Interface Stress Studies

Run Order (Sample IDs)	Temperature	Result
1 (KZ26-1 / KZ28-1)	176F (80C)	No visual damage to either sample
2 (KZ26-2 / KZ28-2)	<545F (285C)	KZ28-2 failed at about 541F (283C) before reaching the target temperature. The failure occurred suddenly with the sample flying off the shelf and landing on the bottom of the oven. The wafers remained intact, so the failure was delamination at one or more of the interfaces between the wafers. The specific interface of the failure was not determined. The test was halted immediately after failure occurred. KZ26-2 showed that delamination began with the wafers separating in one quadrant.
3 (KZ26-3 / KZ28-3)	320F (160C)	No visual damage to either sample.
4 (KZ26-5 / KZ28-5)	<392F (200C)	KZ26-5 failed at about 325F (163C) before the reaching target temperature. The failure occurred suddenly with the sample flying off the shelf and landing on the bottom of the oven (similar to KZ28-2). The wafers remained intact, so the failure was delamination at one or more of the interfaces between the wafers. The specific interface of the failure was not determined. The test was halted immediately after failure occurred. KZ28-5 showed no visual damage.
Samples KZ26-4, KZ28-4 remain untested as controls.		

As the results in Table 19 suggest, the performance of the interfaces between the anti-reflection coatings and the adhesive and the interfaces between the anti-reflection coatings and the wafers is variable. This result would seem to confirm the variable nature of the TPV module failures in that some modules fail and others do not at the same temperatures. The conclusion is that isothermal temperatures in the TPV module greater than the fabrication temperature (in all cases room temperature) can cause delamination failure of one or more of the interfaces between the tandem filter and the TPV cell. Furthermore, from the analytical study previously described, the optical adhesive is causing the majority of the interface stress when the isothermal temperature of the TPV module exceeds the fabrication temperature of the module.

Third, Rugate Technologies, Inc. implemented alternative, anti-reflection coatings for the tandem filters that are expected to be more robust than previous anti-reflection coatings. To digress briefly, an anti-reflection coating is applied to the back side (side opposite the incident radiation) of the tandem filter to ensure that the above band gap photons that reach the back surface pass into the optical adhesive and then to the TPV cell for conversion. This anti-reflection coating is at the interface between the tandem filter and the optical adhesive, and a similar anti-reflection coating is at the interface of the optical adhesive and the TPV cell.

For convenience, the previous anti-reflection coating was based on the same materials used for the optical interference coatings on the incident side of the tandem filter. These materials were perceived to have low strength and the potential cause of the postulated delaminations.

As previously stated, the cause of the module failure is uncertain. However, a module failure occurred with the previous anti-reflection coatings and a module failure occurred with the new, robust anti-reflection coatings. Therefore, the alternative, anti-reflection coatings would seem not to have completely eliminated the TPV module failures.

Additional Information

Additional information about the progress since January 2003 is contained in the following of journal articles, conference papers, and conference presentations:

- Journal Articles
    - R. T. Kristensen, J. F. Beausang, and D. M. DePoy, "Frequency Selective Surfaces as Near Infrared Electro-Magnetic Filters for Thermophotovoltaic Spectral Contro”l" *Journal of Applied Physics*, vol. 95, pp. 4845-4851, 2004
    - P. M. Fourspring, D. M. DePoy, T. D. Rahmlow, Jr., J. E. Lazo-Wasem, and E. J. Gratrix, "Optical Coatings for Thermophotovoltaic Spectral Control”, *Applied Optics*, 2006
- Conference Papers
    - P. M. Fourspring, D. M. DePoy, T. D. Rahmlow, Jr., J. E. Lazo-Wasem, and E. J. Gratrix, "Optical Coatings for Thermophotovoltaic Spectral Control”, paper for the Optical Interference Coatings Conference, Tucson, Arizon, USA, June 2004
    - P. M. Fourspring, D. M. DePoy, J. F. Beausang, E. J. Gratrix, R. T. Kristensen, T. D. Rahmlow, Jr., P. J. Talamo, J. E. Lazo-Wasem, and B. Wernsman, "Thermophotovoltaic Spectral Control”, paper for the 6th International Conference on the Thermophotovoltaic Generation of Electricity (TPV6), Frieburg, Germany, July 2004
    - T. D. Rahmlow Jr., J. E. Lazo-Wasem, E. J. Gratrix, P. M. Fourspring, and D. M. DePoy, "New Performance Levels for TPV Front Surface Filters""paper for the 6th International Conference on the Thermophotovoltaic Generation of Electricity (TPV6), Frieburg, Germany, July 2004
    - D. M. DePoy, P. M. Fourspring, P. F. Baldasaro, J. F. Beausang, E. J. Brown, M. W. Dashiell, K. D. Rahner, T. D. Rahmlow Jr., J. E. Lazo-Wasem, E. J. Gratrix, and B. Wernsman, "Thermophotovoltaic Spectral Control”, paper for the International Energy Conversion Engineering Conference, Providence, RI, USA, August 2004

- T. D. Rahmlow Jr., J. E. Lazo-Wasem, E. J. Gratrix, J. J. Azarkevich, E. J. Brown, D. M. DePoy, D. R. Eno, P. M. Fourspring, J. R. Parrington, R. G. Mahorter, and B. Wernsman, "Engineering Spectral Control Using Front Surface Filters for Maximum TPV Energy Conversion System Performance", paper for the International Energy Conversion Engineering Conference, Providence, RI, USA, August 2004

- Conference Presentations

  - D. M. DePoy, J. F. Beausang, P. M. Fourspring, R. T. Kristensen, S. A. Derry, B. Wernsman, T. D. Rahmlow Jr., T. M. Lyszczarz, B. Monk, J. B. Pryor, and J. L. Volakis, "TPV Spectral Control", presented at Direct Energy Conversion Technology (DTEC), December 2003

  - T. D. Rahmlow Jr. and P. M. Fourspring, "New Performance Levels for TPV Front Surface Filters", presented at Direct Energy Conversion Technology (DTEC), December 2003

  - P. M. Fourspring, D. M. DePoy, T. D. Rahmlow, Jr., J. E. Lazo-Wasem, and E. J. Gratrix, "Optical Coatings for Thermophotovoltaic Spectral Control", presented at Optical Interference Coatings, Tucson, Arizon, USA, June 2004

  - P. M. Fourspring, D. M. DePoy, J. F. Beausang, E. J. Gratrix, R. T. Kristensen, T. D. Rahmlow, Jr., P. J. Talamo, J. E. Lazo-Wasem, and B. Wernsman, "Thermophotovoltaic Spectral Control", presented at 6th International Conference on the Thermophotovoltaic Generation of Electricity (TPV6), Frieburg, Germany, July 2004

  - T. D. Rahmlow Jr., J. E. Lazo-Wasem, E. J. Gratrix, P. M. Fourspring, and D. M. DePoy, "New Performance Levels for TPV Front Surface Filters", presented at 6th International Conference on the Thermophotovoltaic Generation of Electricity (TPV6), Frieburg, Germany, July 2004

  - D. M. DePoy, P. M. Fourspring, P. F. Baldasaro, J. F. Beausang, E. J. Brown, M. W. Dashiell, K. D. Rahner, T. D. Rahmlow Jr., J. E. Lazo-Wasem, E. J. Gratrix, and B. Wernsman, "Thermophotovoltaic Spectral Control", presented at International Energy Conversion Engineering Conference, Providence, RI, USA, August 2004

  - T. D. Rahmlow Jr., J. E. Lazo-Wasem, E. J. Gratrix, J. J. Azarkevich, E. J. Brown, D. M. DePoy, D. R. Eno, P. M. Fourspring, J. R. Parrington, R. G. Mahorter, and B. Wernsman, "Engineering Spectral Control Using Front Surface Filters for Maximum TPV Energy Conversion System Performance", presented at International Energy Conversion Engineering Conference, Providence, RI, USA, August 2004

  - T. D. Rahmlow Jr., J. E. Lazo-Wasem, E. J. Gratrix, P. M. Fourspring, and D. M. DePoy, "Front Surface Spectral Control Development for TPV Energy

Conversion", presented at Direct Energy Conversion Technology (DTEC), December 2004

- T. D. Rahmlow Jr., J. E. Lazo-Wasem, E. J. Gratrix, P. M. Fourspring, and D. M. DePoy, "Front Surface, Tandem Filters Using Sapphire (Al2O3) Substrates for Spectral Control in Thermophotovoltaic Systems", presented at Space Technology and Information Forum (STAIF), New Mexico, USA, February 2005

- D. M. DePoy, P. M. Fourspring, H. Ehsani, E. J. Brown, J. J. Azarkevich, T. A. Lavery, P. C. Sander, S. R. Burger, M. W. Dashiell, K. D. Rahner, T. D. Rahmlow Jr., E. J. Gratrix, J. E. Lazo-Wasem, and B. R. Wernsman, "High Temperature Filters for Radioisotope-TPV Space Power Systems", presented at Space Technology and Information Forum, New Mexico, USA, February 2006

REFERENCES

[1] B. Wernsman, R. G. Mahorter, R. R. Siergiej, S. D. Link, R. J. Wehrer, S. J. Belanger, P. M. Fourspring, S. Murray, F. Newman, D. R. Taylor, and T. D. Rahmlow Jr., "Advanced Thermophotovoltaic Devices for Space Nuclear Power Systems," presented at Space Technology and Applications International Forum - STAIF 2005, New Mexico, USA, 2005.

[2] B. Wernsman, R. R. Siergiej, S. D. Link, R. G. Mohorter, M. N. Palmisiano, R. J. Wehrer, R. W. Schultz, G. P. Schmuck, R. L. Messham, S. Murray, C. S. Murray, F. Newman, D. Taylor, D. M. DePoy, and J. Thomas D. Rahmlow, "Greater than 20% Radiant Heat Conversion Efficiency of a Thermophotovoltaic Radiator / Module System Using Reflective Spectral Control," *IEEE Transactions on Electron Devices*, vol. 51, pp. 512-515, 2004.

[3] P. W. Baumeister, *Optical Coating Technology*, first ed: SPIE Press, 2004.

[4] D. M. DePoy, M. W. Dashiell, K. D. Rahner, L. R. Danielson, J. E. Oppenlander, J. L. Vell, and R. J. Wehrer, "Analysis of TPV Network Losses," presented at Direct Energy Conversion Technology (DTEC) 2004, 2004.

[5] Personal Communication, J. Oliver, 2003.

[6] H. A. Macleod, *Thin-Film Optical Filters*, Third ed. Bristol and Philadelphia: Institute of Physics Publishing, 2001.

[7] E. D. Palik, *Handbook of Optical Constants of Solids*: Academic Press, 1985.

[8] L. M. Hanssen and S. G. Kaplan, "Methods for Absolute Reflectance Measurement of Transmissive Materials in the Infrared," presented at SPIE, San Diego CA USA, 1998.

[9] J. R. Birch and F. J. J. Clarke, "Fifty Categories of Ordinate Error in Fourier Transform Spectroscopy," *Spectroscopy Europe*, vol. 7, pp. 16-22, 1995.

[10] S. G. Kaplan and L. M. Hanssen, "Angle-Dependent Absolute Infrared Reflectance and Transmittance Measurements," presented at SPIE, 2000.

[11] L. M. Hanssen, "Integrating-sphere System and Method for Absolute Measurement of Transmittance, Reflectance, and Absorptance of Specular Samples," *Applied Optics*, vol. 40, pp. 3196-3204, 2001.